Australian Government
Department of Defence
Science and Technology

Investigation of the ElectroPuls E3000 Testing Machine for Fatigue Testing of Structural Materials

Lucy Caine and Emily Frain

Maritime Division
Defence Science and Technology Group

DST-Group-TR-3319

ABSTRACT

An investigation into the use of the Instron ElectroPuls E3000 for the purpose of fatigue crack growth rate testing of structural materials was conducted. The reference material used in this study was BIS812EMA steel and fatigue testing was performed in accordance with ASTM E 47-13. The ElectroPuls E3000 produced fatigue crack growth rate data (at a frequency of 10 Hz) that was consistent with previous testing performed on servo-hydraulic testing machines (at a frequency of 2 Hz). The apparatus was able to produce reliable data up to a frequency of approximately 40 Hz; the exact frequency limit depended on the R-ratio of the cyclic loading. An attempt was made to measure the threshold stress intensity factor range for BIS812EMA. The results indicate that for an R-ratio of 0.5, the threshold stress intensity factor range is approximately 3.2 MPa·m^{½}. Limitations of the test apparatus were identified under certain test conditions, for example, undershoot of the minimum load at high frequencies.

RELEASE LIMITATION

Approved for public release

Published by

Maritime Division
Defence Science and Technology Group
506 Lorimer St
Fishermans Bend, Victoria 3207 Australia

Telephone: 1300 333 362
Fax: (03) 9626 7999

AR-016-750
December 2016

APPROVED FOR PUBLIC RELEASE

Investigation of the ElectroPuls E3000 Testing Machine for Fatigue Testing of Structural Materials

Executive Summary

An investigation into the applicability of the Electropuls E3000 test machine and associated apparatus for fatigue crack growth testing of structural materials was conducted. The Electropuls E3000 is an electrically actuated test machine that claims to be able to operate at frequencies "over 100 Hz" and has the potential to increase efficiency by decreasing test time, as compared with a servo-hydraulic test machine that, typically, has a maximum operating frequency of 10 Hz. The aims of the investigation were (i) to ensure that the ElectroPuls E3000 produced data consistent with previous testing, and (ii) to investigate any specific problems or technicalities of the test machine, associated apparatus, and software operation. Fatigue testing was performed in accordance with ASTM E 647-13 *Standard Test Method for Measurement of Fatigue Crack Growth Rates*. The reference material used in this study was BIS812EMA steel. This material was selected as its fatigue behaviour has been well characterised.

The ElectroPuls E3000 produced fatigue crack growth rate data (at a frequency of 10 Hz) that was consistent with previous testing performed on servo-hydraulic testing machines (at a frequency of 2 Hz). Fatigue striation measurements obtained through quantitative fractography using a scanning electron microscope were consistent with results of other steels detailed in the literature. The ElectroPuls E3000, associated test apparatus, and software produced reliable data up to a frequency of approximately 40 Hz; the exact frequency limit depended on the R-ratio of the load cycle. Capitalising on the higher frequency capability of the apparatus and corresponding reduced test duration, an attempt was made to produce threshold stress intensity factor range data for BIS812EMA. This parameter had not been previously characterised for this material. For an R-ratio of 0.5, the threshold stress intensity factor range was approximately 3.2 MPa·m½. However, it is recommended that this threshold test be repeated to confirm this result.

Through the course of investigating the behaviour of the test apparatus, limitations were identified under certain conditions, for example, undershoot of the minimum load was observed at high frequencies. Consequently, it is recommended that the high frequency load cell is used to verify small loads at high frequencies. It has been demonstrated that the ElectroPuls E3000 can, with due care, be successfully used to obtain crack growth rate data on structural materials at frequencies greater than those achievable on servo-hydraulic test machines.

Authors

Lucy Caine
Aerospace Division

Lucy Caine is a final year university student completing a combined Bachelor of Engineering and Bachelor of Arts at Monash University, majoring in Materials Engineering. Lucy completed this project as part of the DST Group's Student Vacation Scholarship program. Currently, Lucy is working in the Aircraft Forensic Engineering Task as a participant in the Industry Experience Placement Program at the DST Group.

Emily Frain
Maritime Division

Emily Frain completed a combined Bachelor of Engineering and Bachelor of Science (Hons) with Physics and, Mechanical and Materials Systems majors at the Australian National University in 2008. Since 2009 she has worked as an engineer/scientist in the Armour Mechanics and Vehicle Survivability Group and the Structural Materials and Fabrication Group of the Maritime Division of the DST Group. In this time she has contributed to full scale vehicle survivability tests and characterisations and mechanical testing of naval materials.

Contents

Abbreviations

ΔK	stress intensity factor range
ΔK_{th}	threshold stress intensity factor range
$\sigma_{0.2\%}$	yield stress, stress at 0.2% strain
σ_{UTS}	ultimate tensile strength
a	crack length
a_{notch}	specimen notch length
ASTM	American Society for Testing and Materials
B	specimen thickness
C_g	normalised K-gradient
COD	crack opening displacement
CT	Compact Tension
da/dN	crack growth rate
dadN	Software package used for monitoring test parameters
DST Group	Defence Science and Technology Group
h	specimen notch height
K_{max}	maximum stress intensity factor
P_{max}	maximum load applied over a cycle
P_{min}	minimum load applied over a cycle
R	ratio of maximum load applied to the minimum load applied over a cycle
R-ratio	ratio of maximum load applied to the minimum load applied over a cycle
SCE	saturated calomel electrode
W	specimen width

This page is intentionally blank

1. Introduction

1.1 Fatigue Testing

Fatigue is a damage process that can occur in structures that are subjected to cyclic loads, where the loading level is usually macroscopically below that required for the gross yielding of the part [1]. That is, the remote stresses in the part are less than the yield strength of the material. However, due to characteristics of the part or material, such as, surface irregularities, internal flaws, or microstructural features, there are locations where the local microscopic stress exceeds the yield strength during the loading cycle, resulting in local plastic deformation. Continual application of the cyclic load can lead to deformations of sufficient size to initiate a crack, which can then advance during the tensile stress part of the cycle [1]. Fatigue cracks are accompanied by very little gross plastic deformation and normally grow over a lengthy period of time. Fatigue cracks are detrimental since once the fatigue crack has grown to a sufficient size, the remaining material will not be able to support the load of the following cycle and fracture will occur [1]. This final fracture is usually catastrophic [1]; thus, it is important to understand the loads and conditions that will lead to the initiation and propagation of fatigue cracks in a structural material in order to effectively predict and monitor fatigue within a structure. Fatigue crack growth data are obtained by subjecting a laboratory specimen to cyclic loading [2]. There is similitude between the crack in the laboratory specimen and a crack in a structure if the two crack tip stress fields are identical [2]. Accordingly, the results from the laboratory test can be used to analyse crack growth in the structure.

One method used to characterise the fatigue behaviour of a material is through linear elastic fracture mechanics, using the concepts of crack growth rate and stress intensity factor range. Fatigue crack growth data is often presented as a relationship between the crack growth rate ($^{da}/_{dN}$) and stress intensity factor range (ΔK) (Figure 1). The crack growth rate ($^{da}/_{dN}$) is the length by which the crack (with length "a") has increased over a single loading cycle – the units are typically mm/cycle. The stress intensity factor range (ΔK) of a crack in a material describes the change in the local stresses at the crack caused by the cyclic stresses applied to the component as a whole. ΔK is dependent on specimen geometry, the size and location of the crack, and the magnitude and stress ratio of the cyclic load. ΔK is often expressed with units of $MPa \cdot m^{1/2}$.

The typical $^{da}/_{dN}$ versus ΔK curve has three distinct regions. Region I, which corresponds to low stress intensity factor ranges, is associated with threshold behaviour [3]. In Region I the crack growth rate becomes increasingly slow and impractical to measure[1] or crack growth does not occur [3]. A threshold stress intensity factor range, ΔK_{th}, has been defined as the stress intensity factor range at which the crack growth rate corresponds to

[1] The time for a measurable increment of crack growth to occur can become days, and, consequently, practical test constraints such as interruption of power supply and machine availability can limit test duration.

10^{-7}mm/cycle[2] [4]. In Region II the crack growth data is approximately linear and the most widely accepted curve fit is the Paris Equation [5] (Figure 1) [3]. The Paris Equation can be used in conjunction with the critical value of stress intensity factor to estimate the number of cycles to fracture [3]. In Region III rapid unstable crack growth occurs [3].

An important variable that influences the behaviour of the entire crack growth curve is the stress ratio, known as the 'R-ratio' or 'R'. The R-ratio is the ratio of maximum load applied (P_{max}) to the minimum load applied (P_{min}) over a cycle ($R = {}^{P_{max}}/_{P_{min}}$). In general, an increase in R-ratio leads to an increase in ${}^{da}/_{dN}$ for each given ΔK [3]. The crack growth rate data will be also be affected by the combination of environment and material. For example, the rate of fatigue crack growth can be an order of magnitude higher in air as compared with a vacuum [2]. The seawater environment can be particularly detrimental to fatigue life, for example, a seawater environment can increase the fatigue crack growth rate of cathodically protected (-1050 mV(SCE)) BIS812EMA steel by up to 16 times [6, 7]. The frequency of the load cycle can also affect the crack growth rate data as it dictates the time available for interaction between the material and the environment. A frequency effect on the fatigue crack growth rate is not present, or very minor, for a material tested in an inert environment [3, 8]. Galsworthy [9] found that there was only a small effect of frequency on crack growth rate in air, as compared with a sea water environment for high strength steels. There are many more factors, such as, loading waveform shape, that influence crack growth rate data so it is prudent to obtain data that is relevant to the in-service conditions when using fatigue crack growth data for prediction [2].

Fatigue is the process of incremental crack growth over numerous cycles. Consequently, fatigue crack growth rate testing of structural materials can be a time-consuming process, especially if the in-service conditions are faithfully simulated or at a stress intensity factor range near the threshold value. One way in which testing times can be shortened is by increasing the frequency with which the cyclic loading is applied. This may be achieved with electrically actuated test machines such as the Instron ElectroPuls E3000. However, there is the potential that this increase in frequency may affect the crack growth rate, and, consequently, the results will be less applicable to in-service loading where cyclic frequencies are lower.

In this present study, fatigue testing has been conducted on BIS812EMA steel (which is used as the Collins class submarine hull material), in the laboratory air environment, using the ElectroPuls E3000 to evaluate the suitability of this machine for future testing of high-strength submarine steels. Tests were performed to establish the crack growth behaviour of this material in the linear (Region II) and threshold (Region I) regions. The results were compared with results from previous testing which was conducted using the servo-hydraulic Instron testing machines, under the same environmental conditions.

[2] For a cyclic frequency of 10 Hz and a measured crack growth increment of 0.1 mm, one data point would be generated every 1.2 days once the crack growth rate is 10^{-7} mm/cycle. It would take over 10 days to produce a single data point once the crack growth rate has reduced to 10^{-8} mm/cycle.

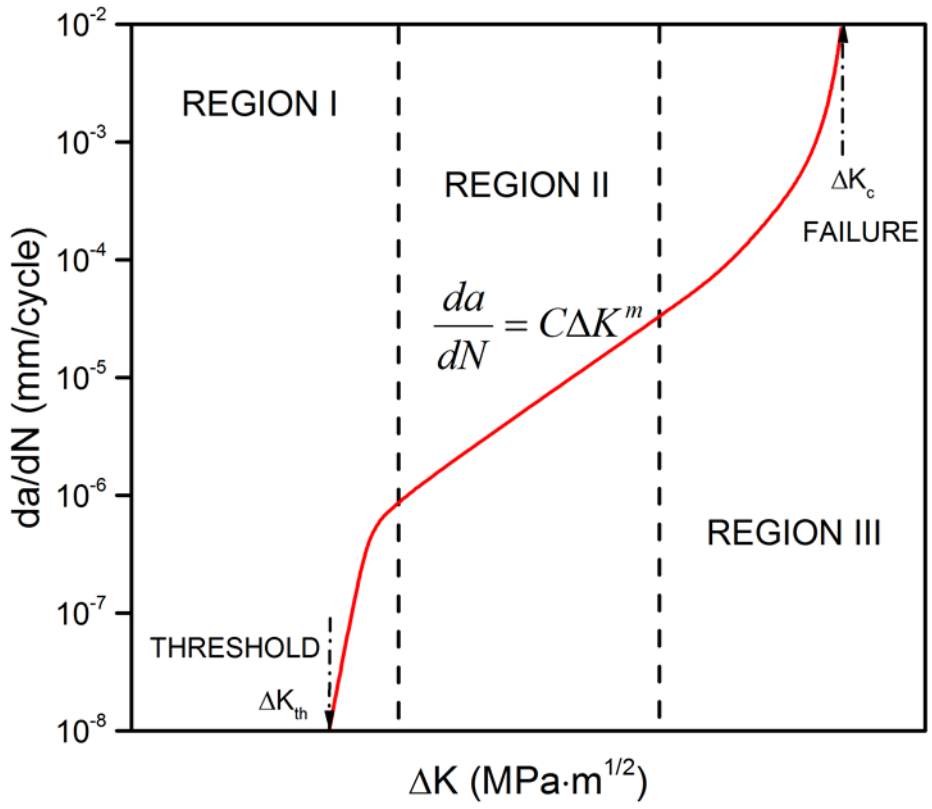

Figure 1 Characteristic curve for fatigue crack growth rate - consisting of three regions of distinct crack growth rate behaviour [10]. Also shown is the Paris Equation that is applicable to Region II of the crack growth rate curve [5].

1.2 Formation of Fatigue Striations

Striations are a common characteristic of the fracture surfaces produced by fatigue crack growth. The generally accepted mechanism for crack growth and striation formation during fatigue crack growth involves crack advancement and blunting during loading, followed by re-sharpening of the crack tip and deformation of a portion of the newly formed surface (the surface created during loading portion of the cycle) during unloading [11]. Crack advance and blunting probably involves dislocation activity around the crack tips [11] as shown diagrammatically in Figure 2. The appearance and profile of striations can vary widely, depending on the material, ΔK, the R-ratio, environmental conditions and other variables [11]. Striation appearance can even be different in adjacent regions of the same fracture surface [11].

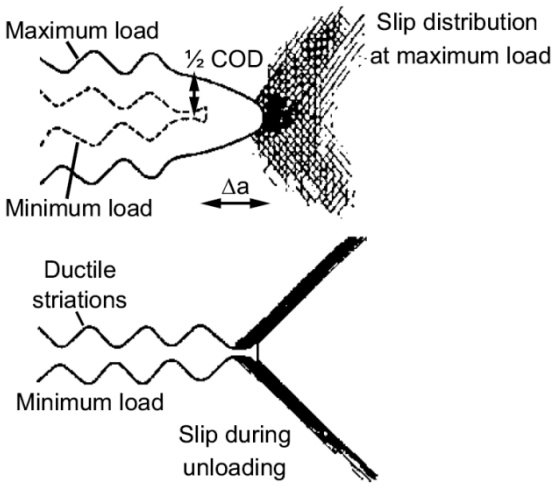

Figure 2 Formation of ductile fatigue striations in an inert media (diagram from [8])

1.3 Instron ElectroPuls E3000

Many machines used for fatigue testing are servo-hydraulic. Typically, these machines are limited to operating at frequencies of up to approximately 10 Hz. This limits the optimisation of test times. At extremely low ΔK values, testing time can be long in duration due to the very small crack growth increment per cycle. Thus, the length of a test is highly dependent on the frequency available to the machine. While optimising test duration is desirable, it is important to have an understanding of the effect of cyclic load frequency on crack growth rate behaviour. It is with these factors in mind that the Instron ElectroPuls E3000 is being considered for fatigue testing of structural materials. The manufacturer specifications for this all-electric test machine stipulate that it has a maximum load capacity of 3 kN and claim an operational frequency of "over 100 Hz". In contrast, many servo-hydraulic machines have significantly greater load capacity, for example, 100 kN or greater.

2. Project Aims

The overall aim of this project was to investigate the use of the Instron ElectroPuls E3000 test machine for fatigue testing. This project assessed the operational limitations of both the machine and the provided Instron software ("dadN") for constant amplitude fatigue crack growth testing. In addition to this, an attempt was made to investigate concerns that measurements would be inaccurate at higher frequencies. This involved ensuring that the test machine produced data that met the requirements laid out in the fatigue testing standard ASTM E 647-13 *Standard Test Method for Measurement of Fatigue Crack Growth Rates* [4], and was able to produce data that showed good agreement with data previously collected from other test machines (such as Instron servo-hydraulic testing machines). The reference material used in this study for comparison was BIS812EMA steel, since its fatigue behaviour has been well characterised.

3. Materials

BIS812EMA is the high-strength low-alloy steel used as the hull-plate steel in the Collins Class submarines. It has small numbers of micro-alloying elements that serve to increase the low temperature toughness of the material. Further increases in toughness are gained through a quenching and tempering heat treatment process, resulting in a tempered martensitic microstructure[3] (Figure 3). The composition and typical mechanical properties of BIS812EMA are shown in Table 1 and Table 2, respectively.

Table 1 Typical chemical composition of BIS812EMA (values are weight percent unless specified otherwise)

	C	Si	Mn	P	S	Cr	Ni	Mo	V
Typical [13]	0.13	0.24	0.93	0.01	0.002	0.48	1.28	0.39	0.02
	Ti	Cu	Al	Nb	B	N	Ca	O	Fe
Typical [13]	0.01	0.21	0.07	0.01	0.007	*	3 ppm	0.009	Balance

* Not recorded

Table 2 Typical mechanical properties of BIS812EMA plate

	Yield stress, $\sigma_{0.2\%}$ (MPa)	Ultimate tensile strength, σ_{UTS} (MPa)	Elongation (A5, %)
Typical [13]	750	840	18

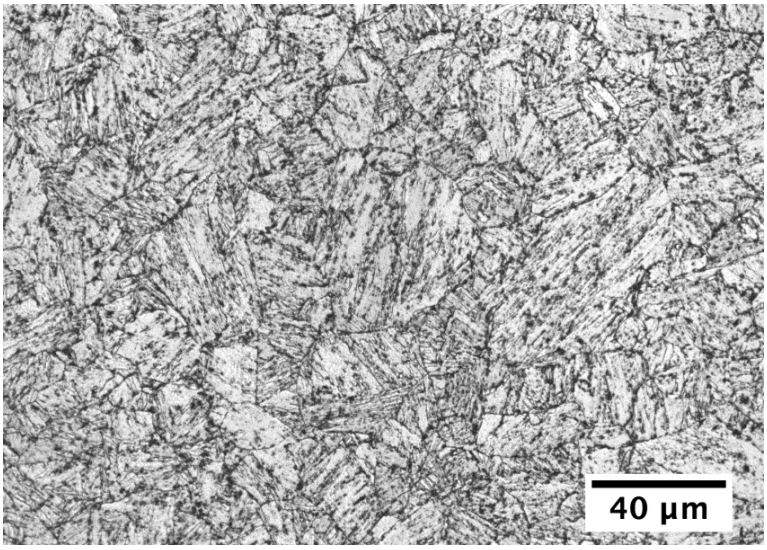

Figure 3 Optical micrograph (brightfield) showing a polished and etched (acidified ferric chloride etchant) section of BIS812EMA steel [14]. BIS812EMA is a quenched and tempered steel with a martensitic structure.

[3] In contrast, un-tempered martensite is a high-strength material that is too brittle to be of use for submarine-hull applications. The tempering process enhances the ductility and toughness of the material with minimal loss of strength [12].

4. Experimental Procedure

4.1 Test Setup

The ElectroPuls E3000 test machine (Figure 4) is situated in a laboratory air environment, where the relative humidity cannot be controlled but is monitored — generally falling between 20 and 50 %. Self-aligning grips were designed and machined for the ElectroPuls E3000, so as to ensure that the specimens only underwent uniaxial tension. Clevises were manufactured according to section A1.4 of ASTM E 647-13 [4]. An MTS Crack Opening Displacement (COD) gauge was used to measure crack growth using the compliance method for all testing. Over the course of this project, the test set-up was operated at frequencies up to and including 40 Hz, though it should be noted that this was not attempted at full load capacity.

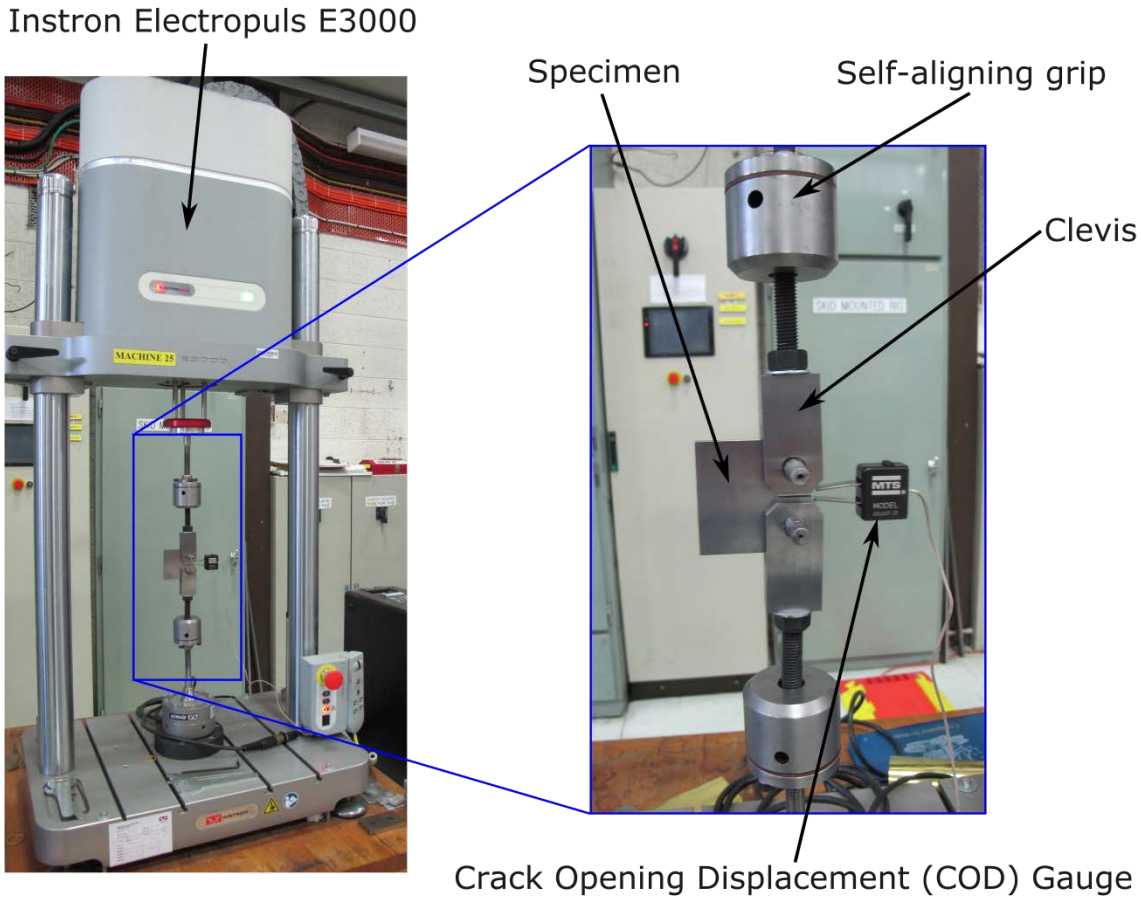

Figure 4 Instron ElectroPuls E3000 testing machine, in place at DST Group, Melbourne and the load line test set-up for this project.

4.2 Fatigue Crack Growth Testing

Testing was carried out in compliance with ASTM E 647-13 [4]. In this standard, fatigue crack growth tests are used to determine the crack growth rate ($^{da}/_{dN}$) corresponding to the stress intensity factor range (ΔK) at the crack tip.

4.2.1 Specimen Geometry

In ASTM E 647-13 [4], three different specimen geometries are outlined – of these, the Compact Tension (CT) specimen was chosen (Figure 5). This specimen has the advantage of requiring the least amount of test material to evaluate the crack growth behaviour. The coupons were machined from finished plate, and, therefore, no residual stresses from welding or machining of the notch are expected to exist. Residual stresses in coupons can lead to greater scatter than otherwise expected in the results (see ASTM E 647-13 section 5.1.4 for details).

The specimens were cut from 35 mm thick plate. The rolling direction of the plate was not marked on the plate. Consequently Charpy impact tests were performed to identify the rolling direction. The result, included in Appendix A, indicated that the CT specimens are oriented in the TL direction in accordance with standard fracture toughness labelling convention shown in Figure 6. All fatigue specimens tested in this study were of the same orientation (TL).

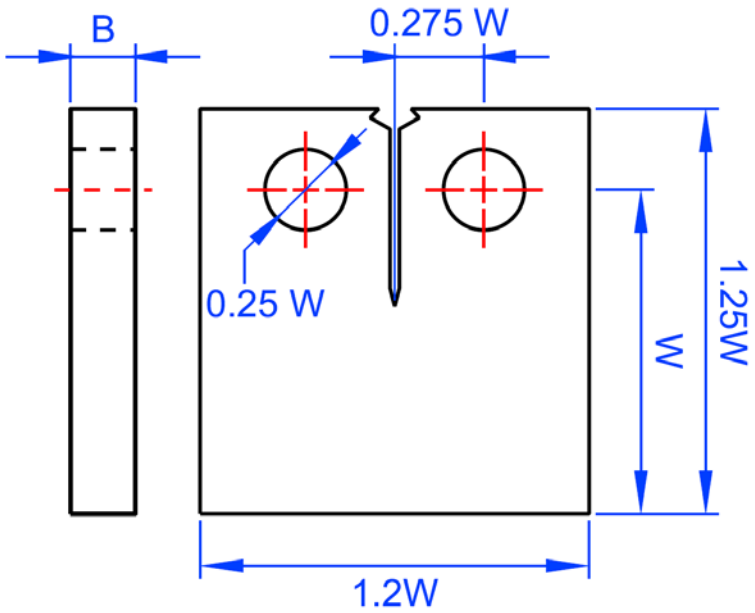

Figure 5 Relative dimensions of the Compact Tension (CT) specimen, as described in ASTM E 647-13 [4], where thickness (B) = 5 mm, width (W) = 50 mm, and the notch length (a_{notch}) was the minimum described in the standard for the width, such that a_{notch} = 0.2×W = 10 mm.

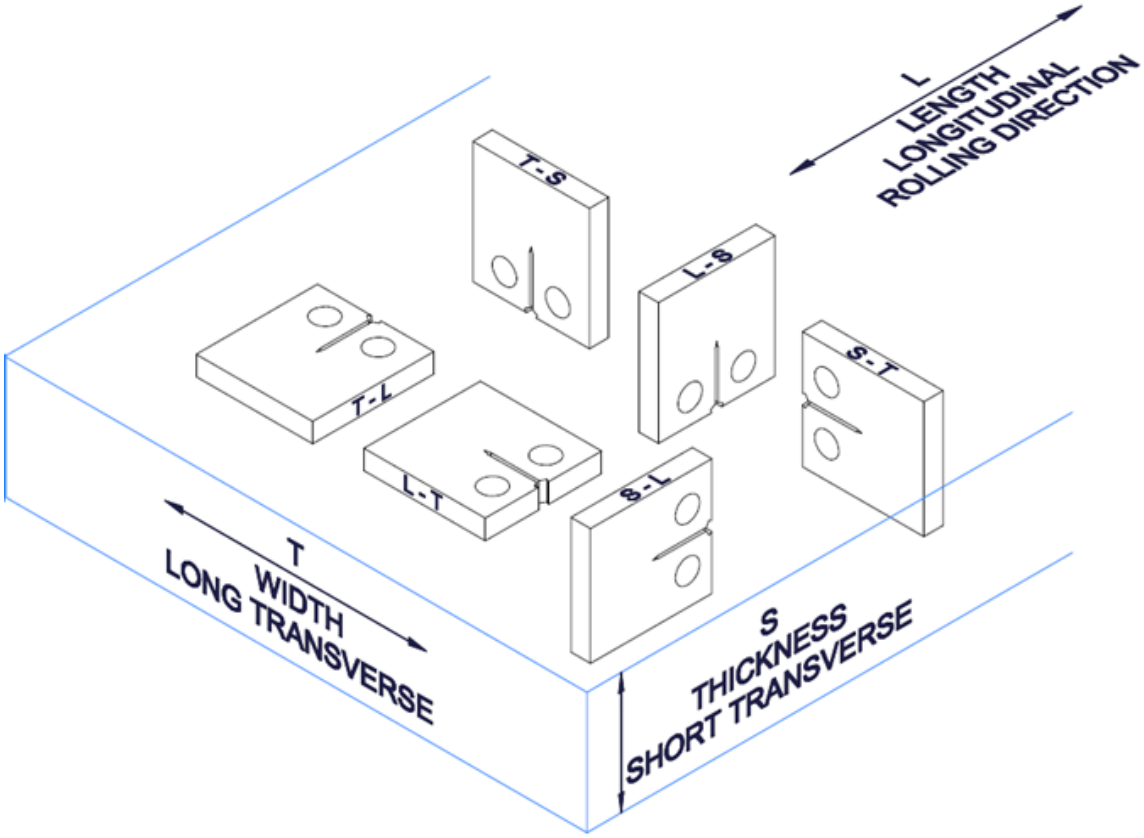

Figure 6 The naming conventions for Compact Tension (CT) specimens sectioned from plate metal. The specimens used in this project were all TL.

4.2.2 Pre-cracking

ASTM E 647-13 requires that the notched specimen be pre-cracked in order to produce a sharpened, straight crack, from which testing can proceed. Pre-cracking was performed in accordance with ASTM E 647-13. Pre-cracks were grown to be not less than "0.1B, *h*, or 1.00 mm, whichever is greater" (where *h* refers to the height of the notch). For the specimens used in this study, this corresponded to a minimum pre-crack length of 1.55 mm. Pre-cracking could not be performed on the ElectroPuls E3000, due to the low maximum load capacity of this machine. Consequently, pre-cracking was performed on a 100 kN Instron Servo-Hydraulic testing machine. An important consideration during the pre-cracking process is that the size of the final plastic zone formed by pre-cracking can affect the crack growth rate in subsequent testing. To eliminate this effect, the final maximum stress intensity factor, K_{max}, of the pre-cracking process was matched to the initial K_{max} of the subsequent test.

4.2.3 ΔK-Increasing Tests

A ΔK-increasing test was performed to confirm previous findings of region II behaviour, and to ensure that the ElectroPuls E3000 could closely replicate previous testing. This test is dependent on the normalised K-gradient (C_g). This factor dictates the rate at which force is increased or shed as a function of the current length of the crack (Equation 1). The normalised K-gradient (C_g) for these tests was 0.04 mm^{-1}. Testing consisted of applying increasing cyclic loading to the test specimen. An initial ΔK of 12.2 $MPa \cdot m^{½}$ and an R-ratio of 0.1 was used. The rate at which force is increased or shed in a fatigue test is given by Equation 1.

$$\Delta K = \Delta K_o exp\left(C_g(a - a_o)\right)$$

Equation 1

where, ΔK_o and a_o are the initial stress intensity factor range and the initial crack length for the test, respectively.

4.2.4 Threshold Tests

Two ΔK-decreasing tests were performed, in the same manner as ΔK-increasing tests described above. This was done not only to add to the available data pool by finding threshold stress intensity factor (ΔK_{th}) values of the material (ΔK_{th} has not previously been measured for BIS812EMA), but also to investigate the performance and precision of the ElectroPuls E3000 at low loads. Testing consisted of applying decreasing cyclic loading to the test specimen. The first test was performed at R-ratio of 0.1, and the second at an R-ratio of 0.5. The normalised K-gradient (C_g) for these tests was -0.08 mm^{-1}.

4.2.5 Constant-ΔK Tests

Constant-ΔK tests were performed to ensure that the accuracy of data (such as the compliance measurement of crack length, which is the basis for calculation of crack growth rate) was not significantly impaired at higher frequencies. In addition to this, it was useful to evaluate the frequency limitations of the apparatus (for specimens of this geometry). This was identified by noting those frequencies at which compliance readings could not be taken. A sequence of constant-ΔK tests were carried out at a ΔK of 10 and 20 $MPa \cdot m^{½}$, at an R-ratio of 0.1, and at a ΔK of 11 $MPa \cdot m^{½}$ for an R-ratio of 0.5. It was expected that the crack growth rate for each ΔK would remain relatively constant.

5. Results

5.1 ΔK-Increasing Tests

5.1.1 ElectroPuls E3000 Test Data

The results of the ΔK-increasing (and of one ΔK-decreasing) test are shown in Figures 7 and 8. Figure 7 shows the data plotted with a Paris Equation fit to the data. The data obtained during the present study exhibits linearity over the ΔK range from 5 to 30 MPa·m^{½}. Figure 8 shows the data plotted with (i) similar data obtained during testing performed at a frequency of 2 Hz on a servo-hydraulic test machine, and (ii) with a scatter band of ± two standard deviations associated with a Paris Equation using constants for fatigue crack growth of ferritic steels with yield strength less than 600 MPa in air [15]. The work by King (1998) to review the literature data for fatigue crack growth rates in steels, for air and seawater environments, contributed to the recommended fatigue crack growth laws described in BS 7910:2005, *Guide to methods for assessing the acceptability of flaws in metallic structures* [16].

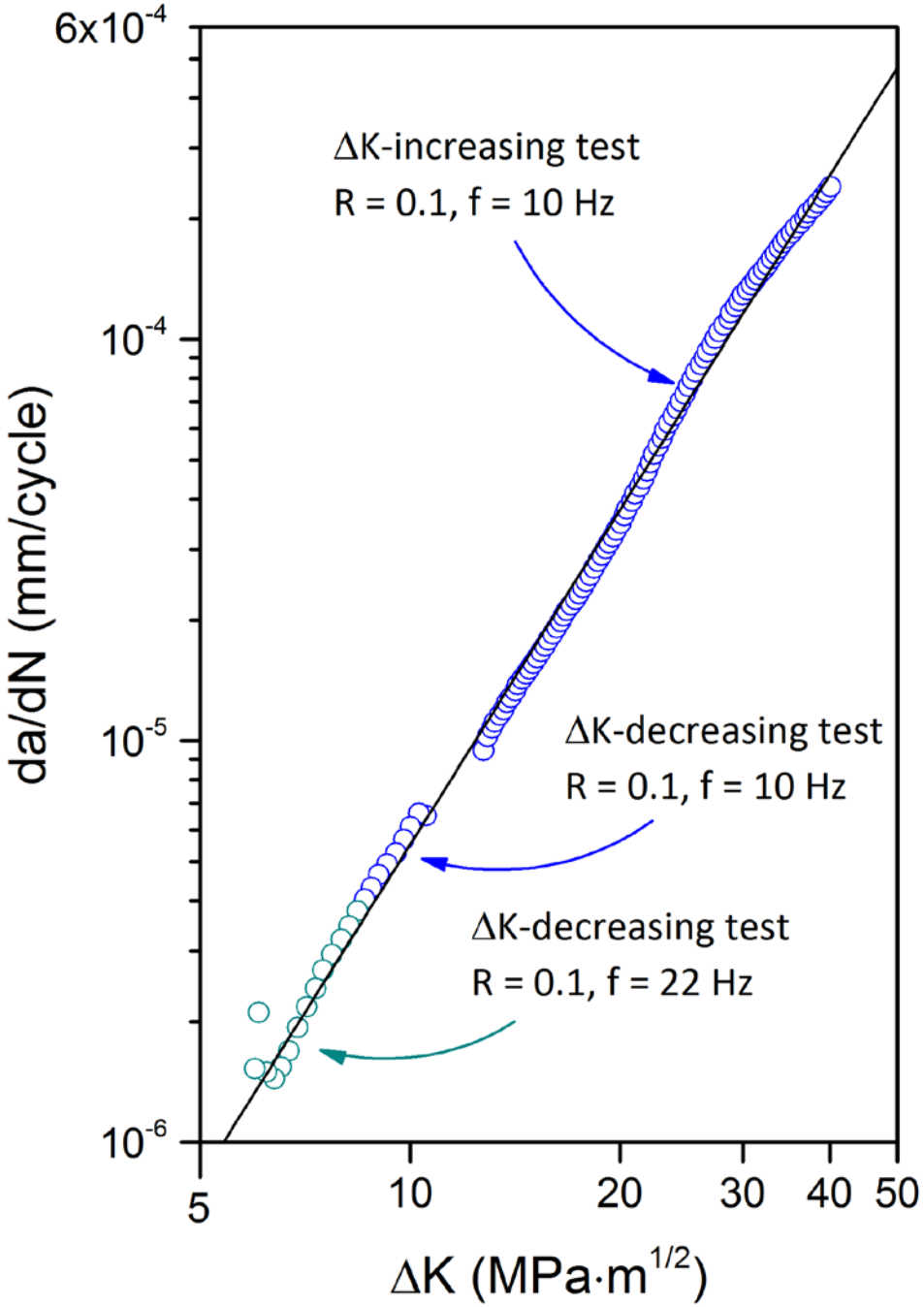

Figure 7 BIS812EMA crack growth rate (da/dN) versus stress intensity factor range (ΔK) data for a ΔK-increasing test (specimen BIS-AB-01) and a ΔK-decreasing test (specimen BIS-AB-04) superimposed on a Paris Equation fit to the data (dashed line).

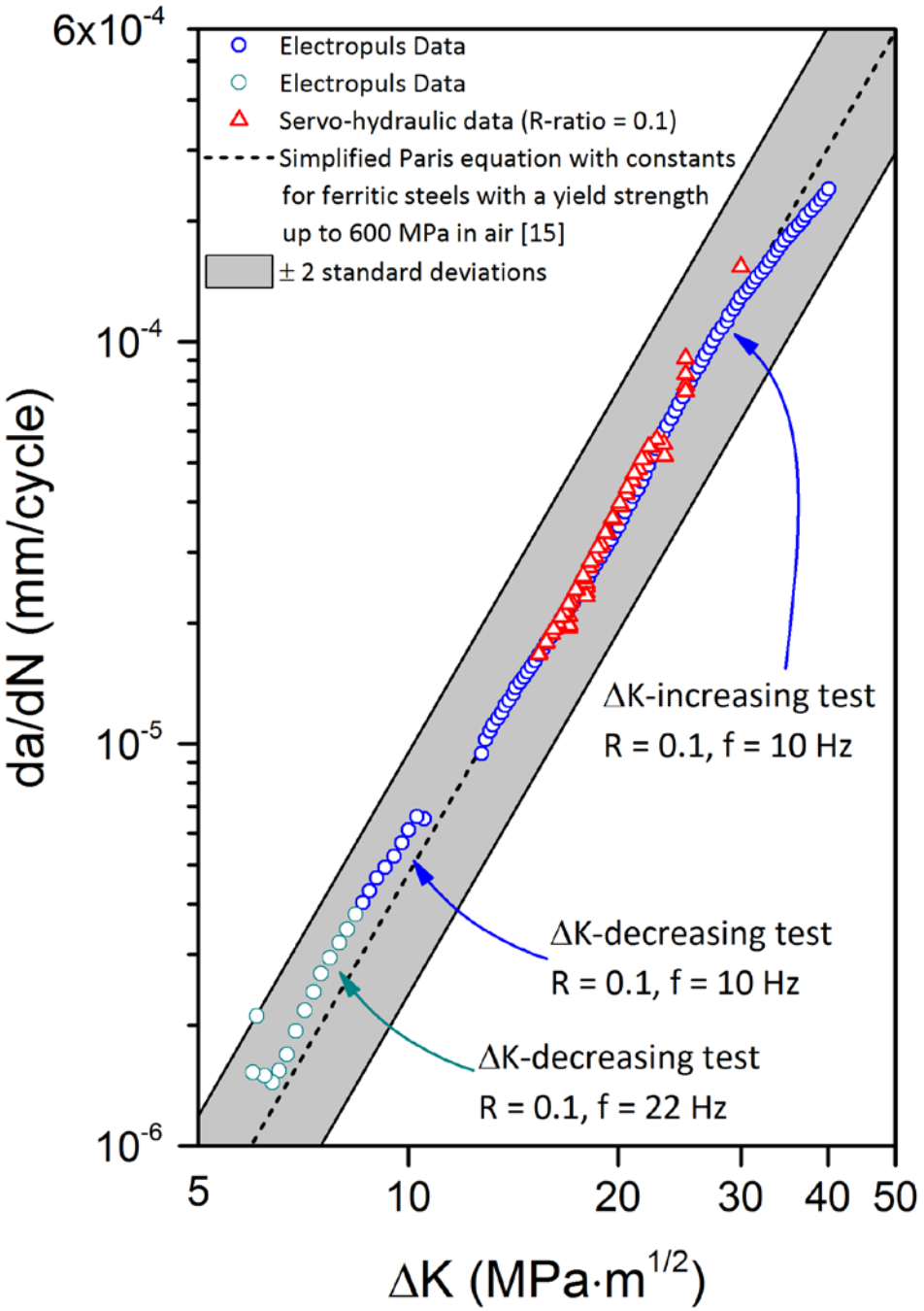

Figure 8 BIS812EMA crack growth rate (da/dN) versus stress intensity factor range (ΔK) data for a ΔK-increasing test (specimen BIS-AB-01) and a ΔK-decreasing test (specimen BIS-AB-04) plotted with (i) previous servo-hydraulic testing machine data of the same steel type (welded) [6] and (ii) a ± two deviation scatter band associated with a Paris Equation fit using constants for fatigue crack growth of ferritic steels with yield strength less than 600 MPa in air [15].

5.1.2 Striation Measurements

Fatigue crack growth is characterised by the presence of microscopic "fatigue striations" on the fracture surface. To count striations on the test specimen, the fracture surface was roughly divided into four even sections (for which the striation spacing was assumed to be regular). Within each of these sections, an attempt was made, using scanning electron microscopy, to locate two clear "runs" of at least ten striations suitable for measurement. A typical striation run is shown in Figure 9(a). The complexity of the fracture surface topography and the difficulty in locating a suitable run of striations is apparent in lower magnification images of the same location (Figures 9(b) and 9(c)).

The results of the striation counts for the specimen, which was subject to a ΔK-increasing test, starting at a ΔK of 12.17 MPa·m^{½}, are listed in Table 3. An estimate of the crack growth rate, using the assumption that each striation corresponds to a single load cycle, is included in these results. The crack growth rate estimate based on the number of striations has been plotted with crack growth rate data obtained during the ΔK-increasing test and data from the literature (Figure 10).

Table 3 Results of striation measurements performed on the fracture surface of a BIS812EMA sample that was subject to a ΔK-increasing test.

Location of "run" along fracture surface (mm)	ΔK at "run" according to test record (MPa·m^{½})	Number of striations counted	Length of striation "run" (mm)	Estimated crack growth rate based on striations measurement (mm/cycle) (x10^{-4})
15.49	12.8	48	0.01030	2.15
16.03	12.8	30	0.00257	0.855
18.16	13.8	105	0.01082	1.03
31.95	23.9	48	0.00797	1.66
31.73	23.9	52	0.00920	1.77
38.73	31.6	59	0.01068	1.81
38.73	31.6	92	0.02463	2.68
38.59	31.6	50	0.00843	1.69

The crack growth rate results based on striation measurements do not reflect the measured crack growth rate recorded during the tests (Figure 10). The crack growth rate estimates based on striations spacing measurements are greater than the crack growth rate calculated from test data, with the difference diminishing as ΔK increases. At a ΔK of approximately 30 MPa·m^{½} the crack growth rate estimate based on striations count begins to coincide with the crack growth rate from the test record.

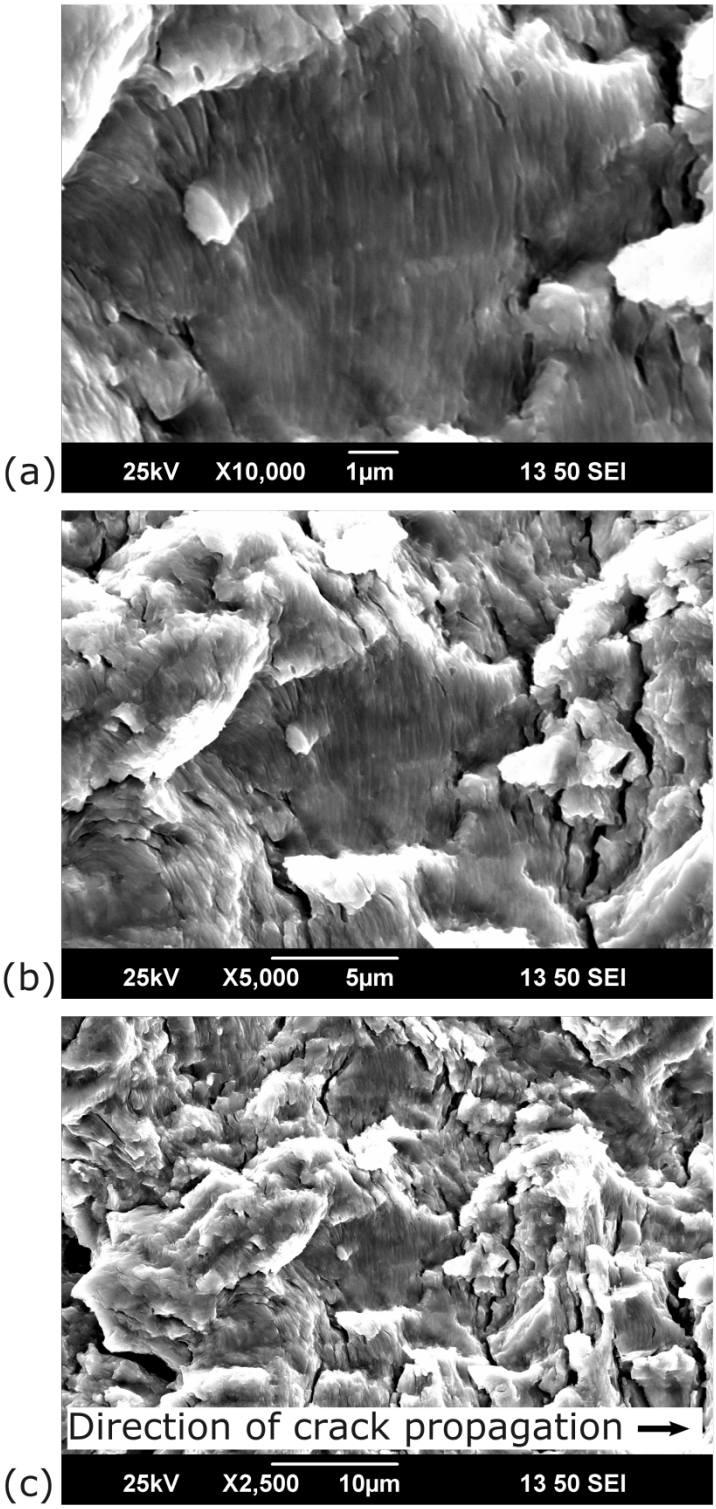

Figure 9 Scanning electron microscopy images showing the fatigue fracture surface of a BIS812EMA specimen viewed at three magnifications: (a) 10,000 times magnification showing a "run" where striations could be identified and counted, (b) 5,000 and (c) 2,500 times magnification showing the complex topography of the fracture surface surrounding the "run" demonstrating the small and isolated nature of the patch.

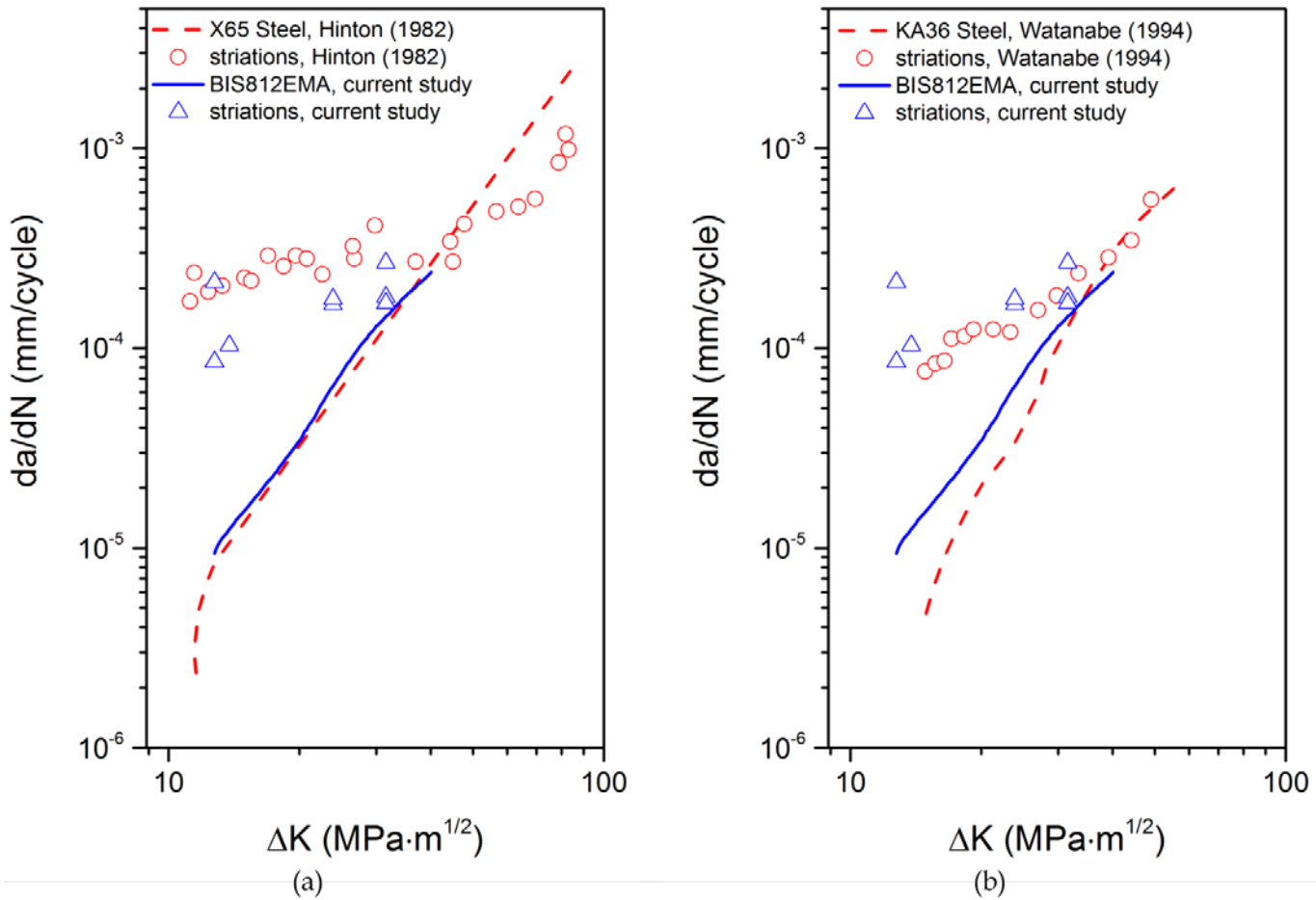

Figure 10 Comparison between crack growth rate data obtained using compliance measurements of crack length and estimates of crack growth rate made from striation spacing measurements, assuming a 1:1 correspondence between striations and cycles. (a) Comparison of BIS812EMA steel data (this study) with X65 steel data from Hinton (1982)[17]. (b) Comparison of BIS812EMA data with KA36 steel data from Watanabe (1994) [18]. Note that below approximately 30 MPa·m½, the crack growth rates estimates based on striation spacing do not decrease with further reductions in ΔK for the Hinton data, the Watanabe data and the data from the current study.

5.2 Threshold Tests

The standard defines ΔK_{th} as the ΔK value that corresponds to a crack growth rate of 10^{-10} m/cycle (10^{-7} mm/cycle). Approximations of ΔK_{th} were obtained for R-ratios of 0.1 and 0.5. Tests were performed at 22 Hz to minimize test time, and were ceased before threshold was reached, due to project time constraints. In the R-ratio of 0.5 experiment, the test was allowed to proceed until the crack growth rate decreased to 1.1×10^{-7} mm/cycle. However, for the R-ratio of 0.1 experiment, the test was halted at a crack growth rate of 2.5×10^{-7} mm/cycle due to the time constraints of the current project. For the R-ratio of 0.5 test, there is a strong trend indicating that ΔK_{th} will be around 3.2 MPa·m^{½}. The result of the R-ratio of 0.1 test was less conclusive, but did indicate that the ΔK_{th} was approximately 4 MPa·m^{½}. Repeat testing would be required to confirm these values.

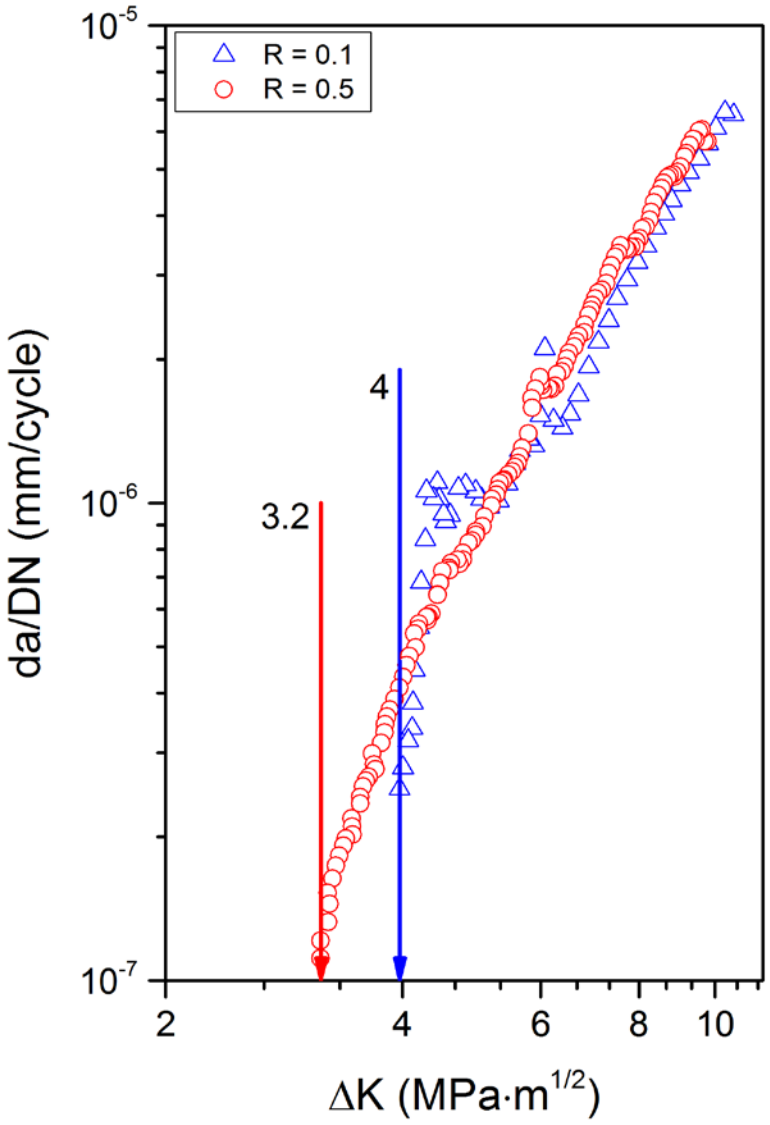

Figure 11 Results of ΔK-decreasing tests, showing trends towards a ΔK_{th} of 3.2 MPa·m^{½} for an R-ratio of 0.5 and a ΔK_{th} of 4 MPa·m^{½} for an R-ratio of 0.1.

5.3 Constant-ΔK Tests

At the high frequencies investigated, it was expected that minimal environmental effects of frequency would be observed, especially considering the tests were performed in air. Any alteration to $^{da}/_{dN}$ that was observed as the frequency changed must, therefore, be related to the performance of the test set-up.

To check for variability in $^{da}/_{dN}$ as a result of cyclic load frequency, a single crack was grown 2 mm at various combinations of load cycle frequencies (10, 20, 30, 36, and 40 Hz), R-ratios (0.5 and 0.1), and stress intensity factor range (10 MPa·m½, 11 MPa·m½ and 20 MPa·m½). The results from these tests are given in Figure 12, plotted with a ± two standard deviation scatter band associated with the results of tests performed at 2 Hz on servo-hydraulic testing machines with the corresponding R-ratios and ΔKs [6].

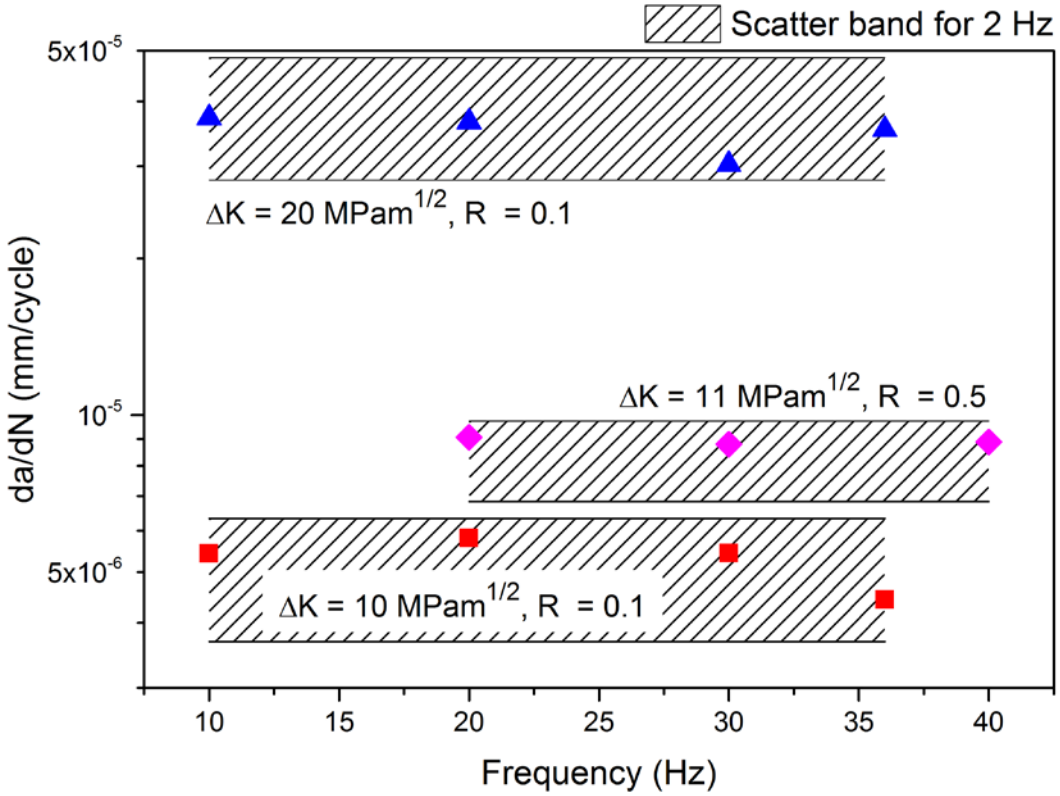

Figure 12 Crack growth rate (da/dN) versus frequency in BIS812EMA for multiple combinations of ΔK and R-ratio tested on the ElectroPuls E3000, compared with a ± two standard deviation scatter band associated with tests performed on BIS812EMA at 2 Hz on servo-hydraulic testing machines.

5.3.1 Compliance Reading Errors

The crack length of the specimen was monitored using the compliance method. This method involves the use of a Clip-on displacement gauge to monitor the opening of the crack, also called the crack opening displacement (COD), in response to the applied load. During the unloading cycle, the gradient of the load versus COD curve is used to calculate the length of the crack. The crack length is monitored over time to generate crack growth rate data. The compliance method can lead to erroneous estimates of crack length in certain situations, for example, if the constraints on crack length and specimen geometry outlined in the ASTM standard are not adhered to, or if the load versus COD curve is not linear (possibly due to crack closure effects). The crack length and the load versus COD curve were qualitatively monitored, during the constant ΔK tests, for deviations from the expected or normal behaviour in order to avoid erroneous readings. It was observed that, whilst testing with an R-ratio of 0.1, erroneous compliance measurements of crack length occurred at a frequency of 36 Hz and greater. Furthermore, at frequencies near to 40 Hz and above, the test apparatus experienced vibration in the load line, and the dadN software reported successive compliance errors and automatically terminated the test. For an R-ratio of 0.5, the erroneous compliance measurements of crack length began to occur at 40 Hz, and the load line vibration, compliance errors and test termination was encountered at frequencies of 45 Hz and greater. Errors were occasionally encountered at frequencies below these identified limiting frequencies; consequently, error inducing frequencies were avoided during testing. Furthermore, an effort was made to characterise the operating envelope of the apparatus to identify conditions where the performance of the machine was optimal (Appendix B).

6. Discussion

6.1 Region II Behaviour

The results of the tests conducted in this study are indicative of Region II fatigue behaviour. Figure 7 shows that the behaviour can be described by the Paris Equation. In addition, the data is consistent with previous testing of the same material and data from the literature for steels tested in air (Figure 8). This testing demonstrated that the ElectroPuls E3000 was able to reproduce crack growth rate data tested on servo-hydraulic equipment, demonstrating that both the test set-up and the experimental process are suitable for fatigue crack growth testing of structural materials at frequencies achievable by electrically actuated test machines. In this case the test frequencies were 10 Hz and 22 Hz.

6.2 Striation Spacing and Comparisons with the Literature

Theoretically, there is a 1:1 correspondence between striations and cycles [19, 20]; Studies (including [17] and [18]) have confirmed this correspondence, but only for ΔK larger than 35 MPa·m^{½}. Thus, there exists a lower limit to the striation to cycles correspondence rule, below which the spacing between striations is observed to remain constant but the actual crack growth rate continues to decrease. This lower limit occurs at a ΔK of around

35 MPa·m^{½}. The results obtained in this study confirmed this 'plateau' effect on striation spacing. Close agreement between the crack growth rate estimate based on striation spacing and measured crack growth rate occurred above 35 MPa·m^{½}, but not below this value (Figure 10). The striation spacing results obtained using the ElectroPuls E3000 test machine are consistent with results and observations made in the literature.

The estimated crack growth rates in the plateau region ranged from 0.855×10^{-4} to 2.68×10^{-4} mm/cycle. This scatter is caused by the difficulties associated with identifying runs of striations on a steel fracture surface. The visibility of fatigue striations (and, hence, the accuracy of the estimate) on a specimen's surface depends on the loading, environment, and the material itself (including the material's microstructure).

One major difficulty in obtaining an accurate striation spacing estimate for steel samples is that striations, in steel, are typically ill-defined, occurring only in isolated patches. This makes the likelihood of finding a satisfactory "run" small [21]. The complex topography of the fracture surface also means that it is not possible to ensure that a "run" is oriented parallel to the image plane. This may contribute to the scatter in the numbers of striations measured per unit length at locations where the stress intensity factor range was similar. In other structural materials, such as aluminium, striations are often well-defined. Typically, fatigue striations on an aluminium fracture surface appear clearly defined in a regular fashion, with little interference from other topography (Figure 13(a)). In contrast, steel exhibits significantly more interference (Figure 13(b)), hindering the ability to identify striations. However, this difficulty identifying striations on the steel fracture surfaces would not account for the lack of 1:1 correspondence between the two methods of estimating $^{da}/_{dN}$. Instead, it is likely that these results confirm that there is a lower limit to the correspondence rule.

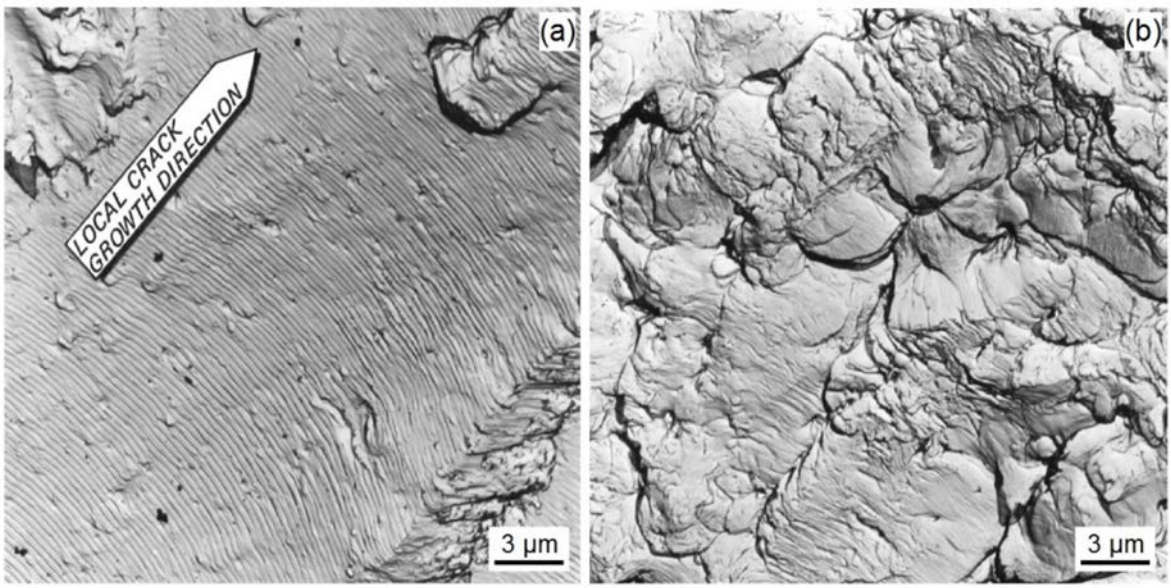

Figure 13: Scanning electron microscopy images of fatigue striation on (a) an aluminium fracture surface and (b) a steel fracture surface (Janssen et al. [10]).

Characterising the appearance of fatigue striations is important to understand fractures that may be encountered in structures. When one looks at a fracture surface and measures the striation spacing it theoretically indicates the amount of crack advancement for each stress cycle. However, if the striation spacing is a value similar to the critical spacing size then there is not necessarily a one-to-one correspondence between the number of striations and the number of stress cycles. Consequently, the actual crack growth rate could be significantly lower than that inferred by a count of the striation spacing. Similarly, where striation spacings are observed to be around this critical value it is not possible to infer the ΔK responsible for the crack growth, except to say that the ΔK will be less than a ΔK of around 35 MPa·m^{½} for steels.

6.3 Threshold Behaviour

Threshold testing is one of the most time consuming crack growth rate tests to perform. In this area, the ElectroPuls E3000 has two potential advantages – first, the potential to use high frequencies to reduce test time significantly (at, for example, four times the maximum frequency possible on a servo-hydraulic testing machine) and secondly, the smaller load capacity of the machine offers the possibility of high precision at low cyclic loads, such as those experienced during the ΔK-decreasing threshold test.

It is generally the case that, as the R-ratio is decreased, the effects of crack surface roughness also causes the effective ΔK to decrease, resulting in a lower than expected growth rate near the threshold ΔK. Therefore, two ΔK-decreasing tests were performed, one with an R-ratio of 0.5 and one with an R-ratio of 0.1.

Matsuoka et al. [22] collected threshold data for HT80 steel from several studies, including their own. HT80 is similar to BIS812EMA in that it is also a high-strength, low-alloy steel. In the current program, the test conducted with an R-ratio of 0.5 was ceased at a crack growth rate of 1.1 x 10^{-7} mm/cycle, whilst the test with an R-ratio of 0.1 was ceased at a crack growth rate of 2.5 x 10^{-7} mm/cycle (Figure 11). The BIS812EMA datum for an R-ratio of 0.5 correlates well with the HT80 steel results (Figure 14). In addition the result is within the scatter of fatigue threshold data from the literature. Consequently, there is confidence in this estimate of ΔK_{th} for BIS812EMA steel in air with an R-ratio of 0.5 (i.e. ΔK_{th} is around 3.2 MPa·m^{½}). Repeat tests could add more confidence to this result.

The BIS812EMA datum for an R-ratio of 0.1 lies towards the far end of the scatter in the literature data. This result also falls below the recommended K_{th}, based on statistical analysis of fatigue threshold data for carbon and carbon-manganese steels in air and seawater environments, corresponding to a 97.7% probability of survival [15]. This second BIS812EMA datum (R-ratio = 0.1) is thought to be inaccurate as a result of some potential issue with the test apparatus. An unexpected plateau was observed in the crack growth rate versus ΔK data between 5 and 6 MPa·m^{½} (Figure 11), which is uncharacteristic of a typical curve and may indicate a problem with this particular test. This test needs to be repeated before a more definitive estimate of ΔK_{th} for an R-ratio of 0.1 can be made.

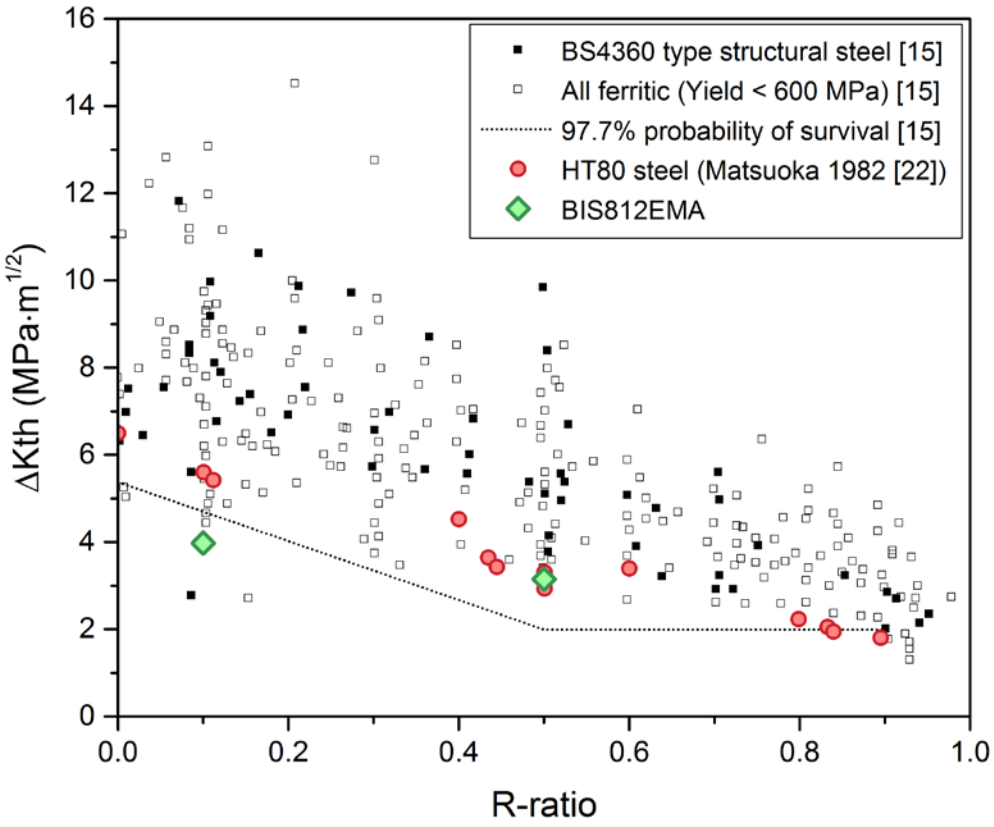

Figure 14 Threshold stress intensity factor range (ΔK_{th}) data points for BIS812EMA (present study), data from the literature [15, 22], and a line corresponding to the "97.7% probability of survival" obtained through statistical analysis of data from the literature for carbon and carbon-manganese steel tested in air and seawater environments (diagram adapted from King [15]).

6.4 Test Frequency Effects

The results of the constant-ΔK tests correlate well with the mean ± two standard deviation scatter band for similar tests conducted at a low frequency (2 Hz) on a servo-hydraulic test machine (Figure 12). This indicates that the ElectroPuls E3000 produced reliable data until an upper limit of frequency was reached.

6.5 ElectroPuls E3000 Testing Considerations & Issues

6.5.1 Sample Size

One important factor to consider when designing a test series that utilises the ElectroPuls E3000 is specimen size. In the case of this project, non-ideal specimen dimensions lead to a significant disadvantage that increased overall testing time significantly. It was found that the length of the CT specimen notch (10 mm, the minimum suggested by the standard for

a width of 50 mm) was too short to allow pre-cracking to occur on the ElectroPuls E3000 in a timely manner since the loads required were too large. Pre-cracking conditions that were found to be suitable were an initial ΔK of 15 MPa·m^{½} and a C_g of -0.08 mm^{-1} (achievable only on a higher capacity servo-hydraulic machine). For these conditions, it took 580000 cycles to grow a 3 mm pre-crack. In contrast, when the initial ΔK used for pre-cracking was 10 MPa·m^{½} (achievable on the ElectroPuls E3000), there was no detectable crack growth after 2.1 million cycles. This was a significant disadvantage as the necessity of first pre-cracking on a slower servo-hydraulic testing machine, and then transferring specimens to the ElectroPuls E3000, led to an increase in overall testing time.

In addition to this, specimen dimensions proved to be a significant limiting factor in achieving a wide ΔK range without the need for very long pre-cracks in some cases. The longer the pre-crack, the shorter the distance available for collection of data – especially when pre-cracking could not be achieved on the ElectroPuls E3000, and, thus, pre-cracking data was not useful for the goal of characterising the machine.

One way in which ElectroPuls E3000 pre-cracking might be achieved for fatigue testing would be by altering the width of the specimens. In ASTM E 647-13, the thickness of the specimen can be within the band of W/20 to W/4. The chosen test specimen width of 50 mm, for example, gives a thickness range of 2.5 mm to 12.5 mm. Specimens at the thinner end of the spectrum tend to require a smaller minimum notch length to achieve a ΔK of 15 MPa·m^{½}, a value at which pre-crack initial was demonstrably possible within a realistic timeframe. It is highly recommended that when considering the ElectroPuls E3000 for fatigue testing using this standard, time be spent modelling the way in which specimen dimension variables will impact the stress intensity factor ranges and the pre-cracking capability of the machine.

6.5.2 Instron dadN Software Limitations

A limitation that was identified for the dadN software was that it can accept a maximum of 5000 data points per second. This effectively limits the amount of data that can be collected (the value that you can safely set for "points/cycle" when setting up your test) depending on the frequency. Figure 15 gives the maximum frequency for a given points/cycle value, above which dadN will freeze and cease testing.

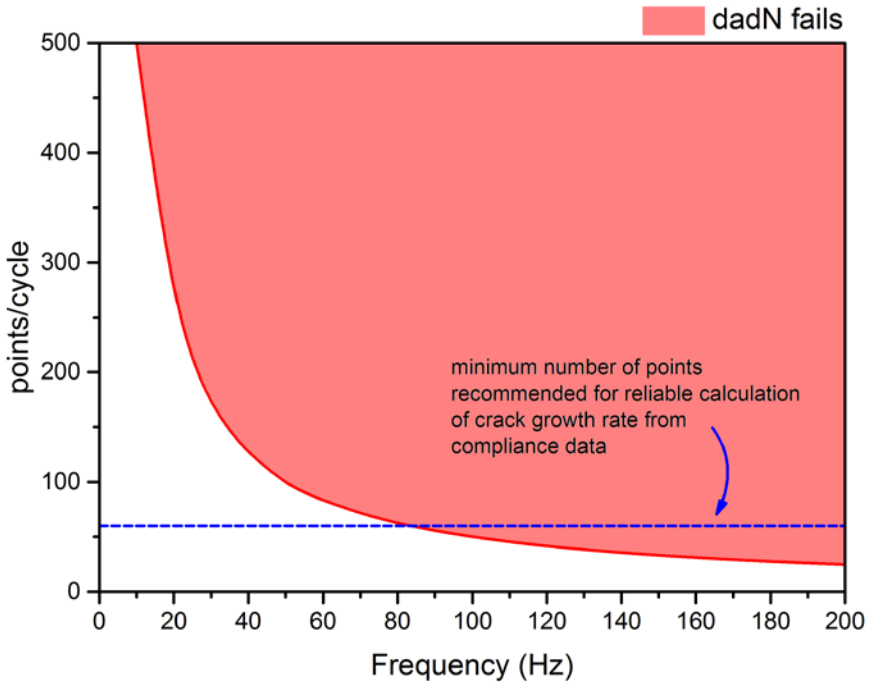

Figure 15 An illustration of the functions limiting the number of points/cycle that can be collected depending on the frequency of testing. These constraints seem to indicate that the maximum frequency achievable with the dadN software on the ElectroPuls E3000 may be approximately 80 Hz.

6.5.3 Frequency and Amplitude Limitations of the Test Apparatus

Through the course of conducting fatigue tests, limiting operational frequencies of the test apparatus were encountered. When the test frequency was raised to these limiting frequencies, vibration was observed in the load line and the test was terminated by the software. This upper frequency limit appeared to depend on the R-ratio and crack length. For example, the constant-ΔK testing found that the Instron ElectroPuls E3000 could be used for fatigue testing at frequencies up to and including 36 Hz at an R-ratio of 0.1, and at up to 40 Hz at an R-ratio of 0.5 (for the crack length present in the specimen, which changed as the test were conducted). In addition, errors were occasionally encountered at isolated frequencies below these identified limiting frequencies; consequently, error inducing frequencies were avoided during testing.

There are several possible explanations for the vibration (shaking) behaviour of the machine. One is that a local resonance is perhaps being encountered somewhere in the load line (i.e. in any part including the grips, clevises, or coupon itself), a theory which is supported by the fact that this shaking behaviour could occur over small isolated frequency intervals (e.g. from 39 to 42 Hz at an R-ratio of 0.5), with normal performance observed at frequencies either greater or less than this interval. This resonance effect could be highly dependent on the shape and mass of the load line elements.

A second possible explanation for the shaking behaviour of the machine is that the machine is failing to apply the specified minimum load of the cycle at high frequencies. This theory is supported by observations made of the load line. The grip and clevis design was such that only a uniaxial tension load could be applied to the specimen. In some instances, a loss of tension was observable as rotation of the clevises with respect to the grips. The loss of tension indicated that the load was reaching zero (i.e., undershooting the minimum specified load of the cycle which was always above 0 N). This effect is more likely to be encountered at low R-ratios (such as 0.1) because the minimum load for this R-ratio passes closer to zero.

Further investigation of these limitations was conducted, detailed in Appendix B, using constant amplitude wave functions at R-ratios of 0.1, 0.5, and 0.9, for maximum loads ranging from 10 to 90 % of the maximum machine capacity of 3000 N (i.e. a P_{max} ranging from 300 N to 2700 N; the P_{min} was then dependant on the R-ratio). Two specimens were used – one in which a crack had not been initiated (notch length was 10.4 mm, measured with an optical traveling microscope), and one with a crack length of approximately 38 mm. Frequency was increased incrementally, and several output variables were qualitatively monitored, these variables were:

- crack length (as measured using the compliance method)
- symmetry and consistency in the wave shape of the applied load (as shown in the dadN software)
- variation and curvature of the load versus COD trace (as shown in the dadN software)
- general behaviour of the load line apparatus (vibration, shaking, etc.).

Deviation of any of these outputs from normal performance (performance at lower frequencies) was recorded. For example, it was noted if the measured crack length changed as a result of change in frequency without the alteration of any other test variable. The results of this investigation are available in Appendix B.

This investigation has led to some guidelines to avoid sub-optimal behaviour of the test apparatus, and, where possible, areas where data measurements are deemed "questionable" in their accuracy. The following issues should be considered when conducting a test using the Electropuls E3000.

1. **Very small crack opening displacement should be avoided, unless using high precision measurement, to avoid compliance errors.**

   It was found that for small crack lengths and small load ranges (specifically, for example, a crack length of 10.4 mm and an R-ratio of 0.9), regardless of the P_{max} and frequency tested, the crack length measurement was not consistent with the expected result. This was most likely due to the very small opening of the crack. The precision of the crack length measurement system (COD gauge[4] and dadN

[4] The clip gauge was an MTS Model 632.02F-20 Clip-on displacement gauge which are designed specifically to meet ASTM E 399 [23] requirements [24]. The gauge's required

software) was not sufficiently precise for crack length measurements when the crack opening displacement was small (less than 0.010 mm). It should also be noted that the clip gauge used had a limit of 50 Hz [24], and, thus, compliance readings gained at frequencies higher than this (if achievable), may not be valid. Tests were not attempted at frequencies greater than 50 Hz. An alternate method of measuring crack length, with higher fidelity, may eliminate this limitation of the test apparatus.

2. **The use of a low minimum load, results in an upper limit on the frequency that can be applied to the specimen. For example, for a load cycle with a minimum load (P_{min}) of 300 N, the maximum frequency for which reliable data will be obtained is approximately 30 to 35 Hz. Accordingly, for minimum loads close to zero, the operator should specify a lower frequency for acceptable data.**

   This limitation of the test apparatus was encountered when varying the load (P_{max}) at an R-ratio of 0.1, for both short and long crack lengths. As the frequency approached 30 to 35 Hz for these conditions, the load train (including the specimen) was observed to rotate. This rotation would only have been possible if there was a loss of tension in the load train. Therefore, it is likely that the self-aligning grips, designed to ensure that any loading applied was fully uniaxial, are losing tension and allowing rotation. This indicates that the machine is undershooting the minimum load at high frequencies, and represents a lower boundary on the precision of the load the machine is able to apply.

3. **Isolated instances of inconsistent crack length measurements were also possible (Figure 16). If a test record contains indeterminate or questionable results, the test should be repeated for a different crack length range on the same specimen.**

   It is possible that these isolated inconsistencies in crack length measurements are a result of some unfavourable combination of maximum load, R-ratio, and crack length that results in a resonance. For example, an isolated inconsistent crack length measurement occurred in a specimen containing a short crack (a = 10.4 mm) with a cyclic loading varying from 180 N (P_{min}) to 1800 N (P_{max}), corresponding to an R-ratio of 0.1, at a frequency of 15 Hz(Figure 16). At frequencies greater than or less than 15 Hz, the crack length monitored using the compliance method reflected the value measured with optical microscopy (10.4 mm). If a test was conducted that happened to coincide with conditions that lead to inconsistent crack length measurement, the assessment of crack growth rate could be negatively impacted.

   In one of the ΔK-decreasing tests conducted in the threshold investigation portion of this project, unexpected peaks in da/dN versus ΔK were observed between a ΔK of 5 MPa·m^{½} and 6 MPa·m^{½} (Figure 11). It is possible that this was one such instance where inconsistency occurred due to an unfavourable combination of

---

precision is stated as a maximum deviation of ± 0.003 mm (0.0001 in.) from a least-squares-best-fit straight line through its displacement calibration data.

variables. A second test over a different range of crack lengths, or at a slightly different frequency, would be able to confirm or refute this hypothesis.

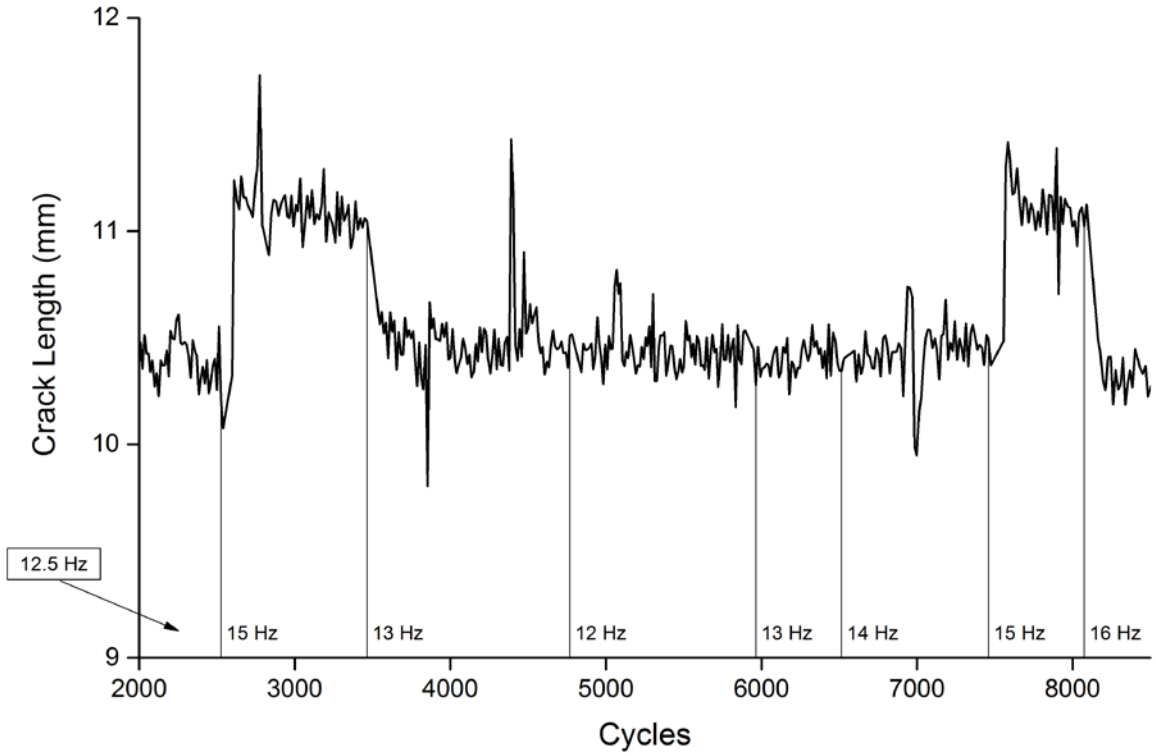

Figure 16 A crack length versus number of cycles plot showing isolated frequencies where inconsistent crack length measurements were encountered. When the frequency was increased from 12.5 Hz to 15 Hz the measured crack length substantially increased (beyond the scatter); once the frequency was reduced to 13 Hz the crack length returned to the nominal value.

7. Conclusions

1. The ElectroPuls E3000 was able to reproduce crack growth rate data obtained from test conducted using servo-hydraulic equipment, demonstrating that both the test set-up and the experimental process are suitable for fatigue crack growth testing of structural materials. However, when using the test apparatus care must be taken to avoid combinations of ΔK, crack length, R-ratio and frequency that can result in spurious measurements.

2. The threshold stress intensity factor range (ΔK_{th}) measurement for BIS812EMA steel (R-ratio of 0.5) is estimated to be approximately 3.2 $MPa \cdot m^{½}$. This result correlates well with the results for HT80 steel and the literature.

8. Recommendations for Future Work

It is recommended that the ΔK_{th} measurements be repeated to provide greater confidence in the values, and, thus, contribute to the existing body of knowledge concerning the fatigue crack growth behaviour of BIS812EMA steel.

If high frequency tests are required for low R-ratios, it would be advisable to first characterise the load application behaviour of the ElectroPuls E3000 with a high frequency load cell to allow for calibration of the undershooting phenomenon. With such a calibration, it would be possible to specify a load cycle for which testing will be accurate at low R-ratios and high frequencies.

9. Acknowledgements

This work was completed as part of a Student Vacation Scholarship and, accordingly, the authors would like to thank the DST Group executive for supporting the Student Vacation Scholarship program.

The authors would like to acknowledge the guidance, planning, and support of Joseph Dominguez. Additionally, thanks are extended to Mark Knop for his patience, willingness to explain concepts and contributing his time and expertise to facilitate the pre-cracking and testing on a servo-hydraulic test machine. Thanks goes to the whole of the Structural Materials and Fabrication Systems work group (Maritime Division) for both their warm welcome and their valuable feedback at various stages of this project. The work could not have been completed without access to the facilities operated and managed by Bruce Crosbie and maintained by Aerospace Division. The authors would also like to acknowledge Rohan Byrnes, for enabling the SEM fractography in this project by contributing his time and expertise to educate colleagues in SEM use.

Appendix A: Charpy Impact Energy Testing

The rolling direction of the plate material used in the present study was not marked on the plate. Consequently Charpy impact energy tests were performed to identify the rolling direction. The plate was nominally assigned an 'A' and a 'B' direction and the CT specimens were all such that the fracture plane was perpendicular to the 'A' direction and the direction of crack propagation was parallel to the 'B' direction, thus, according to standard fracture toughness labelling conventions the specimens were given the designation 'AB'. In addition to the CT specimens, three standard sized Charpy impact energy specimens were extracted from the same plate in both the AB and BA specimen orientations. Charpy impact tests were performed on these specimens at -40°C.

Fracture toughness, and correspondingly Charpy impact energy, tends to be higher in the LT orientation as compared with the TL orientation [25]. In addition, Charpy impact testing of BIS812EMA steel recorded that the impact energy of LT orientation specimens was consistently greater than the impact energy of TL oriented specimens at temperature above -60°C [26]. The impact test results (Table A1) indicated that the BA specimen orientation corresponds to the LT and that the AB specimen orientation corresponds to the TL orientation. Accordingly, the evidence indicated that all the CT specimen correspond to the TL orientation.

Table A1 BIS812EMA Charpy impact energy test results

Specimen ID	**Specimen orientation**	**Test temperature (°C)**	**Impact Energy (J)**	***Predicted orientation***
BIS AB CH01	AB	-40°C	187	*TL*
BIS AB CH02	AB	-40°C	201	*TL*
BIS AB CH03	AB	-40°C	198	*TL*
BIS BA CH01	BA	-40°C	241	*LT*
BIS BA CH02	BA	-40°C	233	*LT*
BIS BA CH03	BA	-40°C	235	*LT*

Appendix B: ElectroPuls E3000 limitation mapping

Over certain frequency ranges, which are test parameter dependant, test irregularities occur. These test irregularities include:

- Inconsistent crack length measurement
- Irregular load wave-shape
- Irregular load versus COD trace
- Machine Vibration
- Compliance errors and test termination.

These will be described in greater detail below.

Figure B1 shows observations made of the behaviour of the test apparatus during constant amplitude sinusoidal loading over a range of frequencies for selected test parameters. Testing was conducted on two specimens, one with a blunt machined notch corresponding to a crack length of 10.4 mm (measured with an travelling optical microscope) and the other contained a crack that had been grown to a length of approximately 38 mm. The performance of the apparatus was observed at R-ratios of 0.1, 0.5, and 0.9 with maximum load (P_{max}) values corresponding to 10%, 20%, 30%, 40%, 50%, 60%, 70%, 80%, and 90% of the Electropuls E3000's 3 kN capacity.

The y-axis in Figure B1(a through f) is the load given in terms of P_{max}, expressed as a percentage of the Electropuls E3000 3000N load capacity and in terms of the load range (P_{min} to P_{max}). For example, 100% would indicate a cycle with a P_{max} of 3000 N where the corresponding P_{min} will depend on the R-ratio (P_{min} will be 300 N, 1500 N, and 2700 N for R-ratios of 0.1, 0.5, and 0.9, respectively). The P_{min} and P_{max} values have been indicated in brackets. The x-axis indicates the frequency of the test and observations made of the performance of the apparatus are indicated by the colour and shape of the data point.

Normal performance (indicated by a green circle in Figure B1) corresponded to a sinusoidal appearance of the load cycle, as shown in the dadN software, a crack length value (measured using the compliance method) that matched the known value (i.e., the measured crack length did not change instantaneously with a change in the frequency) and a linear load versus COD trace (also shown in dadN software). The load versus COD trace is the path traced by a load cycle on a plot of load versus COD and is expected to closely resemble a straight line (Figure B2). Crack closure effects can also alter the slope/shape of the load versus COD trace.

At some frequencies the measured crack length differed from the known value (indicated by a grey diamond in Figure B1). This was observed as a sudden shift in the measured crack length as a result of changing the frequency only (Figure 16). There was no other change to test parameters and an actual alteration to the crack length, be it growth or reduction, would be unlikely or impossible, respectively. Figure 16 shows an instance of this unexpected frequency shift. At the beginning of the trace, the frequency was 12.5 Hz and the measured crack length was 10.4 mm, using the compliance method (in agreement

with the optically measured value). The frequency was changed to 15 Hz and the measured crack length abruptly changed to approximately 11.1 mm, then, when the frequency was changed to 13 Hz, the measured crack length returned to 10.4 mm. The same behaviour was observed when the frequency was changed from 14 Hz, to 15 Hz and then to 16 Hz, indicating that something is occurring at 15 Hz that alters the slope of the load versus COD trace and correspondingly affects the crack length measurement. This difference in crack length measurement was often less than 0.3 mm; however, in some instances it resulted in a difference of 0.8 mm between the measured and the known value. Where the difference was small it may be that crack growth rate calculations are only slightly affected, as the crack growth increment is often at least 0.3 mm and the crack growth rate calculation is based on a seven point polynomial fit. However, it would stand to reason that deviations should be recognised and avoided, if possible.

It was also observed that the shape of the load record diverged from the expected sinusoidal appearance, as monitored in dadN, for some frequencies. This observation (indicated by a light green upright triangle in Figure B1) may or may not have been accompanied by an unexpected crack length measurement.

Furthermore, frequencies at which the behaviour of the load versus COD trace was irregular were observed (indicated by an orange downwards triangle in Figure B1). This irregularity of the load versus COD trace was often, but not always associated with an inconsistent crack length measurement and/or an irregular load wave shape.

Another observation of the performance of the apparatus included instances of loud machine noise, often accompanied by poor load wave shape, irregular load versus COD trace and inconsistent crack length measurement (indicated with a dark red hexagon in Figure B1). Finally, the most extreme example of observed apparatus behaviour was successive compliance calculation failure which caused the software to terminate the test (indicated with a red cross in Figure B1).

To aid with understanding of the information contained in these graphs, by way of example, the behaviour of the test apparatus at an R-ratio of 0.1 and with a specimen containing a short crack (a = 10.4 mm) will be described in the following paragraphs (Figure B1(a)).

Where the loads are small, that is, the P_{max} is approximately 10 % to 20 % of the machine capacity; the measurement of the crack length was only reliable for very small frequencies. When higher frequency tests (16 and 18 Hz, for 10 %, and 20 %, respectively) were performed with these load conditions, successive compliance errors were encountered and the test was terminated by the software. The load versus COD trace was irregular at frequencies beyond 10 Hz for 10 % load capacity and 18 Hz for 20 % load capacity. By re-starting the test using the 20 % load capacity conditions and avoiding 18 Hz, the performance of the machine was able to be monitored at higher frequencies; however, reliable performance of the apparatus did not seem to be possible past 18 Hz (20 %). This performance limitation is likely to be linked to the very small crack opening displacement that must be monitored by the COD gage which was less than 0.010 mm. In contrast, the crack opening displacement for the 90 % load capacity condition was 0.050 mm.

Continuing with the example for an R-ratio of 0.1 and a short crack (Figure B2(a)), it was observed that the test apparatus performed reliably up to a limiting frequency that depended on the load signal. For example, at 40 % load capacity the reliable behaviour was observed up until 25 Hz, at 50 % load capacity the reliable behaviour was observed up until 30 Hz and at 90 % load capacity the reliable behaviour was observed up until 20 Hz.

Notwithstanding the above observations, this does not mean that pockets of reliable behaviour were not observed at frequencies greater than the initial observation of unreliable behaviour. As was observed at 90 % load capacity condition, where from 24 Hz to 28 Hz, reliable apparatus behaviour was observed after a frequency range (21 Hz to 24 Hz) associated with instability. A suitable explanation for these somewhat localised frequency ranges associated with a loss of apparatus reliability has yet to be presented beyond that it may be a result of a resonance effect linked to the specimen geometry, the clip gauge characteristics and some particular load and frequency combination.

At high frequencies and low P_{min} (as is the case considering the R-ratio of 0.1) there was evidence of a loss in tension in the load line indicating possible undershoot of the minimum load at high frequencies. Loss of tension in the load train means that the sample is no longer experiencing the loads that were specified.

Each of the graphs in Figure B1 represent the performance of the test apparatus under specific test conditions and notes have been made to highlight broad observations of the behaviour. To characterise the behaviour of the apparatus in full is beyond the scope of the study. However, these results illustrate the importance of careful load and frequency combination selection. Careful monitoring of the test machine for possible compliance errors or other apparatus irregularities is necessary to ensure that the loads applied to the specimen reflect the behaviour specified by the user.

- Reliable compliance data
- Inconsistent crack length measurement
- Irregular wave-shape load record
- Irregular load vs. COD trace
- Machine vibration
- Compliance errors and test termination

Note 1:
Very low ΔP and short crack length results in minimal COD displacement (see table below) rendering compliance method measurement of crack length unachievable.

R	Machine Capacity	COD displacement(mm)
0.9	90%	<0.007
0.9	40%	<0.004
0.5	20%	<0.007
0.1	10%	<0.007

Note 2:
Low Pmin (close to 0N) and high frequency leads to poor reliability of crack growth data, thought to be resulting from loss of tension in the load line

Note 3:
Hysteresis loop degradation

Note 4:
Isolated loss of reliability in crack measurement which could be a result of unfavourable resonance

Note 5:
Machine vibration at isolated frequencies

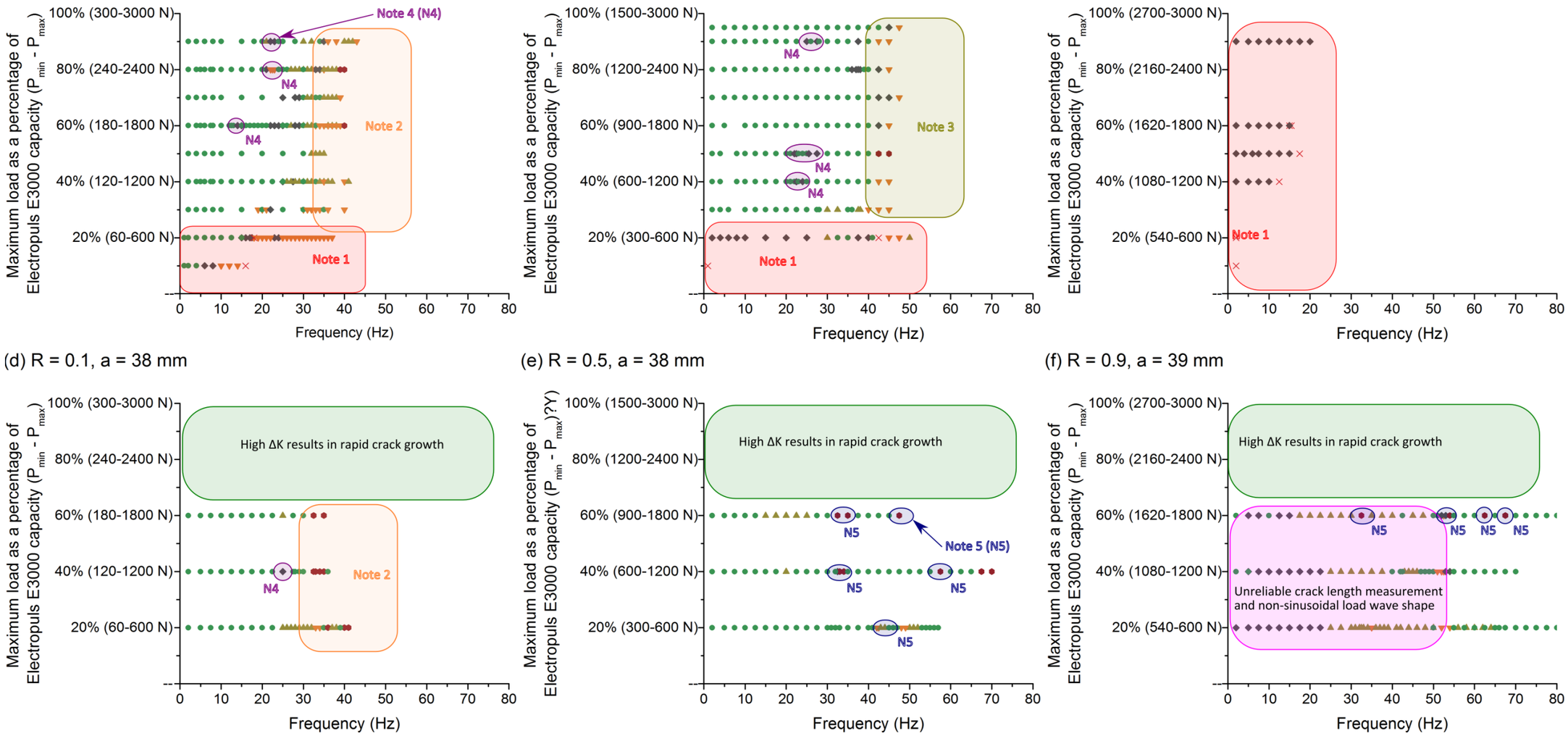

Figure B1 Observations regarding the reliability of the test apparatus for particular test conditions: (a) an R-ratio of 0.1 and a crack length of approximately 10 mm, (b) an R-ratio of 0.5 and a crack length of approximately 10 mm, (c) an R-ratio of 0.9 and a crack length of approximately 10 mm, (d) an R-ratio of 0.1 and a crack length of approximately 38 mm, (e) an R-ratio of 0.5 and a crack length of approximately 38 mm, and (f) an R-ratio of 0.9 and a crack length of approximately 38 mm.

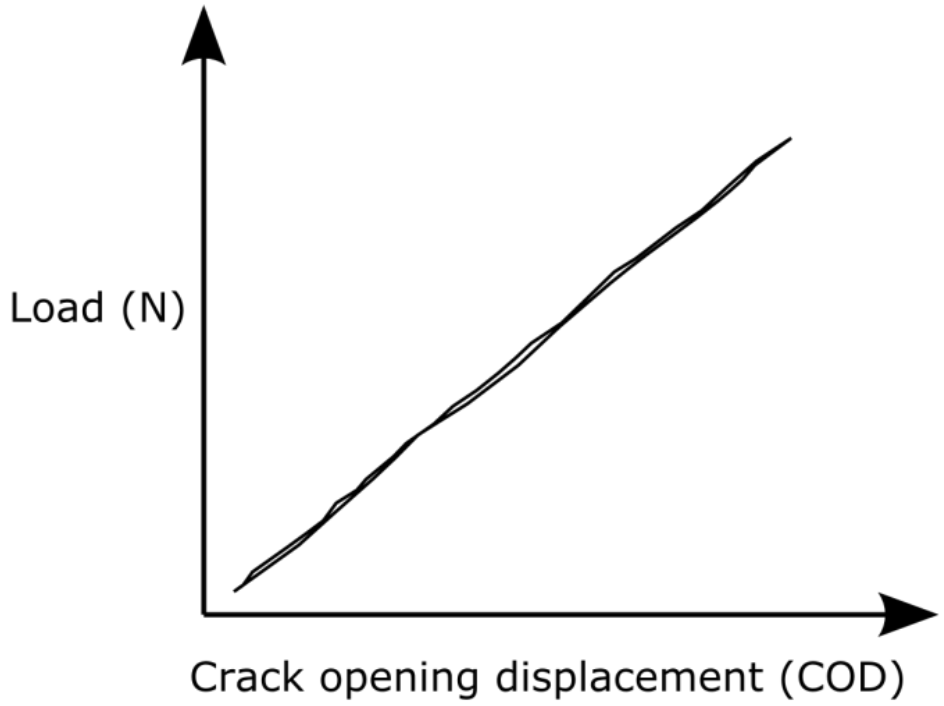

Figure B2 Load versus crack opening displacement (COD) trace indicative of reliable performance of the Electropuls E3000 and associated test apparatus.

References

1. Brooks, C. R. and Choudhury, A. (2002) *Failure Analysis of Engineering Materials*. New York, McGraw-Hill
2. Broek, D. (1989) *The Practical Use of Fracture Mechanics*. Netherlands, Kluwer Academic Publishers
3. Bannantine, J. A., Comer, J. J. and Handrock, J. L. (1990) *Fundamentals of metal fatigue analysis*. Englewood Cliffs, N.J., Prentice Hall
4. *ASTM E 647-13 - Standard Test Method for Measurement of Fatigue Crack Growth Rates*. American Society for Testing and Materials, Pennsylvania, United States of America, 2013.
5. Paris, P. and Erdogan, F. (1963) A critical analysis of crack propagation laws. *Journal of Basic Engineering, Transactions of the American Society of Mechanical Engineers* **December 1963** 528-534
6. Knop, M. (2014) *Unpublished Work*. Defence Science and Technology Organisation.
7. Shah Khan, M. Z. and Burch, I. A. (1992) Effect of seawater on the fatigue life and crack growth behaviour of a new microalloyed steel for submarine hull application. *International Journal of Fatigue* **14** (5) 313-318
8. Lynch, S. P. (1979) Mechanisms of Fatigue and Environmentally Assisted Fatigue. In: *Fatigue Mechanisms, Proceedings of an ASTM-NBS-NSF symposium,* Kansas City, Montana, American Society for Testing and Materials
9. Galsworthy, J. C., *Corrosion Fatigue and Stress Corrosion Cracking (Chapter 4 In: A review of DRA Work on Marine Strength Steels)*. OTO 97 066 [Offshore Technology Report], Health and Safety Executive, Sheffield, UK, 1997.
10. Janssen, M., Zuidema, J. and Wanhill, R. J. H. (2002) *Fracture mechanics*. Delft, DUP Blue Print
11. Lynch, S. P. (2007) Progression markings, striations, and crack-arrest markings on fracture surfaces. *Materials Science and Engineering A* **468-470** 74-80
12. Callister Jr., W. D. (2003) *Material Science and Engineering An Introduction*. Sixth ed, John Wiley & Sons
13. Dixon, B. F. and Taylor, J. S. (1997) Control of Hydrogen Cracking in Collins Class Submarine Welds. In: *Proceedings of the Joint Seminar: Hydrogen Management in Steel Weldments,* Melbourne, Australia: 23 October 1996, Publisher: Organising Committee of the Joint Seminar on behalf of Defence Science and Technology Organisation and Welding Technology Institute of Australia
14. Heath, J. (2012) *Unpublished Research*. Defence Science and Technology Organisation.
15. King, R. N., *A review of fatigue crack growth rates in air and seawater*. OTH 511 [Offshore Technology Report], Health and Safety Executive, Sheffield, UK, 1998.
16. *BS 7910:2005 - Guide to methods for assessing the acceptability of flaws in metallic structures*. British Standards Institution, London, United Kingdom, 2005.
17. Hinton, B. R. W. and Procter, R. P. M. (1982) Quantitative fractography of fatigue cracking of X-65 pipeline steel in air and sodium chloride solutions. *Metals Forum* **5** (1) 80-91
18. Watanabe, E., et al. (1994). Vol. 3, Publ by ASME
19. Connors, W. C. (1994) Fatigue striation spacing analysis. *Materials Characterization* **33** (3) 245-253

20. Khan, Z., Rauf, A. and Younas, M. (1997) Prediction of fatigue crack propagation life in notched members under variable amplitude loading. *Journal of Materials Engineering and Performance* **6** (3) 365-373
21. DeVries, P. H., Ruth, K. T. and Dennies, D. P. (2010) Counting on Fatigue: Striations and Their Measure. *Journal of Failure Analysis and Prevention* **10** 120-137
22. Matsuoka, S., Nishijima, S. and Ohtsubo, S. (1982) Auto ΔK-Decreasing Technique for the Stress Intensity Threshold Level of Fatigue Crack Growth. *Transactions of the Japan Society of Mechanical Engineers. A* **48** (436) 25 December 1982 1505-1513
23. *ASTM E 399-09 - Standard Test Method for Linear-Elastic Plane-Strain Fracture Toughness KIc of Metallic Materials*. American Society for Testing and Materials, Pennsylvania, United States of America, 2009.
24. MTS Systems Corporation. *MTS Services, maintenance parts and accessories catalog for 2015*. [Accessed: 16th February 2015]; Available from: https://www.mts.com/ucm/groups/public/documents/library/dev_003828.pdf
25. Wei, R. P. (2010) *Fracture Mechanics – Integration of Mechanics, Material Science, and Chemistry*, Cambridge University Press
26. Butler, J. J. F., *A metallurgical Evaluation of BIS812EMA*. DRA TM (AWMS) 92239 Defence Research Agency, DRA Dunfermline, Fife, UK, 1992.

DEFENCE SCIENCE AND TECHNOLOGY GROUP DOCUMENT CONTROL DATA	1. DLM/CAVEAT (OF DOCUMENT)

2. TITLE	3. SECURITY CLASSIFICATION (FOR UNCLASSIFIED REPORTS THAT ARE LIMITED RELEASE USE (L) NEXT TO DOCUMENT CLASSIFICATION)
Investigation of the ElectroPuls E3000 Test Machine for Fatigue Testing of Structural Materials	Document (U) Title (U) Abstract (U)
4. AUTHOR(S) Lucy Caine and Emily Frain	5. CORPORATE AUTHOR Defence Science and Technology Group 506 Lorimer St Fishermans Bend Victoria 3207 Australia

6a. DST Group NUMBER	6b. AR NUMBER	6c. TYPE OF REPORT	7. DOCUMENT DATE
DST-Group-TR-3319	AR-016-750	Technical Report	December 2016

8. FILE NUMBER	9. TASK NUMBER	10. TASK SPONSOR	11. NO. OF PAGES	12. NO. OF REFERENCES
			35	26

13. DST Group Publications Repository	14. RELEASE AUTHORITY
http://dspace.DST Group.defence.gov.au/dspace/	Chief, Maritime Division

15. SECONDARY RELEASE STATEMENT OF THIS DOCUMENT

Approved for public release

OVERSEAS ENQUIRIES OUTSIDE STATED LIMITATIONS SHOULD BE REFERRED THROUGH DOCUMENT EXCHANGE, PO BOX 1500, EDINBURGH, SA 5111

16. DELIBERATE ANNOUNCEMENT

No Limitations

17. CITATION IN OTHER DOCUMENTS Yes

18. DST GROUP RESEARCH LIBRARY THESAURUS

Fatigue, BIS812EMA, Striations, High frequency, Crack growth rate

19. ABSTRACT

An investigation into the use of the Instron ElectroPuls E3000 for the purpose of fatigue crack growth rate testing of structural materials was conducted. The reference material used in this study was BIS812EMA steel and fatigue testing was performed in accordance with ASTM E 47-13. The ElectroPuls E3000 produced fatigue crack growth rate data (at a frequency of 10 Hz) that was consistent with previous testing performed on servo-hydraulic testing machines (at a frequency of 2 Hz). The apparatus was able to produce reliable data up to a frequency of approximately 40 Hz; the exact frequency limit depended on the R-ratio of the cyclic loading. An attempt was made to measure the threshold stress intensity factor range for BIS812EMA. The results indicate that for an R-ratio of 0.5, the threshold stress intensity factor range is approximately 3.2 MPa·m^{½}. Limitations of the test apparatus were identified under certain test conditions, for example, undershoot of the minimum load at high frequencies